EFFECT OF SURFACE ROUGHNESS IN MODEL AND FRESH FRUIT SYSTEMS ON MICROBIAL INACTIVATION EFFICACY OF COLD ATMOSPHERIC PRESSURE PLASMA

By

SIDDHARTH BHIDE

A thesis submitted to the

Graduate School-New Brunswick

Rutgers, The State University of New Jersey

In partial fulfillment of the requirements

For the degree of

Master of Science

Graduate Program in Food Science

Written under the direction of

Mukund V. Karwe and Donald W. Schaffner

And approved by

_____

_____

_____

New Brunswick, New Jersey

January 2016

ABSTRACT OF THE THESIS

Effect of Surface Roughness in Model and Fresh Fruit Systems on Microbial Inactivation Efficacy of Cold Atmospheric Pressure Plasma

By SIDDHARTH BHIDE

Thesis Directors: Professor Mukund V. Karwe and Professor Donald W. Schaffner

Cold Atmospheric Pressure Plasma (CAPP) is an ionized gas consisting of charged and neutral particles, and radiation of varying wavelengths. Due to its relatively low temperature, CAPP is considered as a potential non-thermal decontamination technique.

The goal of this research was to assess the suitability of CAPP for fresh produce decontamination as affected by surface roughness. The specific objectives were: i) to isolate and investigate the effect of surface roughness on microbial inactivation efficacy of CAPP using a model system, ii) to understand the extent to which surface roughness affects the microbial inactivation efficacy of CAPP in fresh produce, and iii) to detect and relatively quantify active plasma species in CAPP.

CAPP from filtered dry air was generated using a plasma jet. Optical Emission Spectroscopy (OES) was used to quantify the relative concentrations of plasma species.

Closed coat sandpapers with roughness (quantified via parameter of root mean square deviation Pq, measured using Confocal Laser Scanning Microscopy (CLSM)) ranging from, 6 µm to 16 µm were selected as model system. Sandpapers were inoculated with *Enterobacter aerogenes* (reportedly non-pathogenic, surrogate to *Salmonella* spp), left to dry for two hours, and treated with plasma for eight minutes twelve seconds. Based on their measured Pq values using CLSM, apples, oranges, and cantaloupes surfaces were selected and similar microbial inoculation, processing and analysis were performed.

Model system results showed a 0.52 log higher inactivation of *E. aerogenes* (2.08 log inactivation) on the smoothest sandpaper and the difference was statistically significant from roughest sandpaper. Fruit surfaces results showed 1.25 log higher inactivation on apples (1.86 log inactivation) which were the smoothest and the difference was statistically significant from the roughest cantaloupes. As the surface roughness increased, the microbial inactivation efficacy of CAPP decreased. However, the results from fruit surfaces showed high variability, and were not predictable from the sandpaper data. Emission spectrum from OES indicated the presence of reactive oxygen and nitrogen species with potential to cause microbial inactivation.

In conclusion, microbial inactivation efficacy of CAPP is affected by factors beyond surface roughness and further research is needed to determine its suitability for fresh produce decontamination.

ACKNOWLEDGEMENTS

I take great pleasure in thanking my advisors Dr. Mukund V. Karwe and Dr. Donald W. Schaffner who have guided me with their invaluable inputs and suggestions throughout my graduate studies both on a scientific and a personal front. I have gained tremendously from their expertise in the domains of food engineering and food microbiology.

I would like to thank Dr. Bill Franke for serving on my committee and for guiding me throughout my association with him through Rutgers Food Innovation Center North.

I would like to acknowledge Dr. Deepti Salvi for her invaluable inputs throughout my project, Dave and Bill for setting up the plasma equipment, Dr. Prabhas V. Moghe and Daniel Martin for use of Confocal Laser Scanning Microscopy, Dr. Paul Takhistov for his valuable inputs, Dr. Jim White for allowing me to use Optical Microscopy in his lab, and Dr. Sukanya Murali and Annie D'Souza Palaparthi for helping me out with Scanning Electron Microscopy.

I would take this opportunity to thank all my lab mates from Dr. Karwe's and Dr. Schaffner's lab for their thoughtful suggestions and making the laboratory a friendly and relaxing environment to work in. Last but not the least, I would like to thank my family without whom none of this would have been possible.

TABLE OF CONTENTS

LIST OF FIGURES

LIST OF TABLES

1. INTRODUCTION

1.1 Cold atmospheric pressure plasma (CAPP)

Plasma by definition is the fourth state of matter and consists of partially or wholly ionized gas (Loeb, 1960). When energy is supplied to a solid, the kinetic energy of its constituent molecules increases causing an increase in their relative motions and a transition to liquid state and then gaseous state depending on the amount of energy supplied. If more energy is supplied at this stage (gaseous state), the constituent atoms/molecules start colliding violently and break apart resulting in formation of charged and neutral species like ions, electrons, free radicals, etc., while releasing radiation of varying wavelengths. This mixture of species and radiation is called as plasma. Majority of our universe is in the plasma state and some examples of plasma are lightning, the aurora borealis, and the interior of stars (d'Agostino et al., 2005).

Plasma can be classified based on its temperature into low temperature plasma (LTP) or high temperature plasma (HTP) as shown in Table 1 (Reutscher, 2001). Low temperature plasma is further divided into thermal and non-thermal plasma.

Table 1: Classification of plasma based on temperature

Low Temperature Plasma (LTP)		**High Temperature Plasma (HTP)**
Thermal LTP	**Non thermal LTP**	
$T_g \approx T_i \approx T_e \lesssim 2 * 10^4$ K	$T_g \approx T_i \approx 300$ K ; $T_i << T_e \lesssim 10^5$ K	$T_i \approx T_e > 10^7$ K

(Reutscher, 2001)

Where,

T_g = Temperature of gas molecules

T_i = Temperature of ions

T_e = Temperature of electrons

High temperature plasma (HTP): Plasma is said to be a HTP when the temperature in the system is greater than 10^7 K. At this high temperature, the gas molecules ionize completely giving rise to ions and electrons which collide rapidly and frequently with each other resulting in a thermal equilibrium between the particles and approximately uniform temperature (Zohm, 2005). An example of HTP is fusion plasma like the sun.

Thermal low temperature plasma: Plasma is said to be thermal low temperature plasma when the temperature of the system is less than 2×10^4 K resulting in partial ionization of the gas. However, the temperature is high enough to supply energy to ensure rapid and frequent collision of charged and neutral particles leading to approximately equal temperatures of ions, electrons, and non-ionized gas molecules. An example of thermal low temperature plasma is arc plasma at atmospheric pressure (Reutscher, 2001).

Non-thermal low temperature plasma: Plasma is said to be non-thermal low temperature plasma when the temperature of the system is less than 10^5 K resulting in partial ionization of the gas. In these plasmas, only “few” and “light” electrons reach temperatures of close to 10^5 K whereas the “multitudinous” and “heavier” ions and gas

molecules stay at room temperature (Meichsner, 2005). Thus, the energy and the temperature in the system stay low and there is no frequent collision between the charged and neutral particles. This non-thermal low temperature plasma is referred to as Cold Atmospheric Pressure Plasma (CAPP) when generated at atmospheric pressure and was the focus of this study.

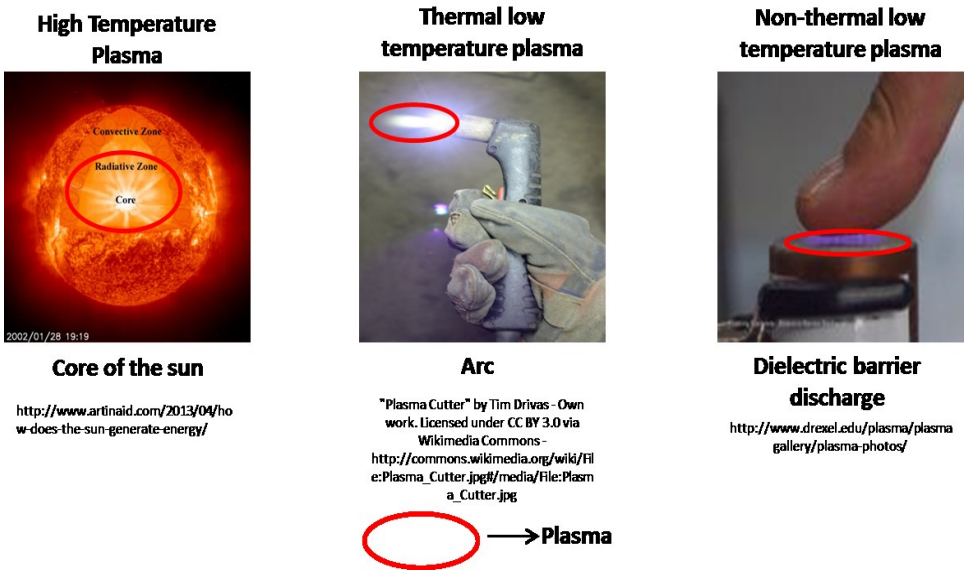

Figure 1: Illustration of different types of plasma

1.1.1 CAPP - Methods of generation

CAPP can be generated in many ways but the four most common generation methods which are reported to be effective against biological contaminants (Ehlbeck et al., 2011) are via dielectric barrier discharge, atmospheric pressure plasma jet, corona discharge, and microwave driven plasmas.

Dielectric barrier discharge (DBD):

DBD plasma is generated by applying a voltage gradient between the two electrodes with one of the dielectric electrodes limiting the discharge current. The passage of current ionizes the gas and leads to generation of plasma between the electrodes. The distance between the electrodes can be varied based on the process need and applied voltage. A variety of different electrode geometries and setups can be made based on the operating need and system. An advantage of using DBD technology is the creation of homogeneous plasma over a large area or volume depending on the electrode geometry. A disadvantage of this mechanism is high ignition voltage of 10 kV or more depending on the electrode gap which requires many precautionary measures (Ehlbeck et al., 2011). Figure 2 illustrates some designs used for CAPP generation by dielectric barrier discharge.

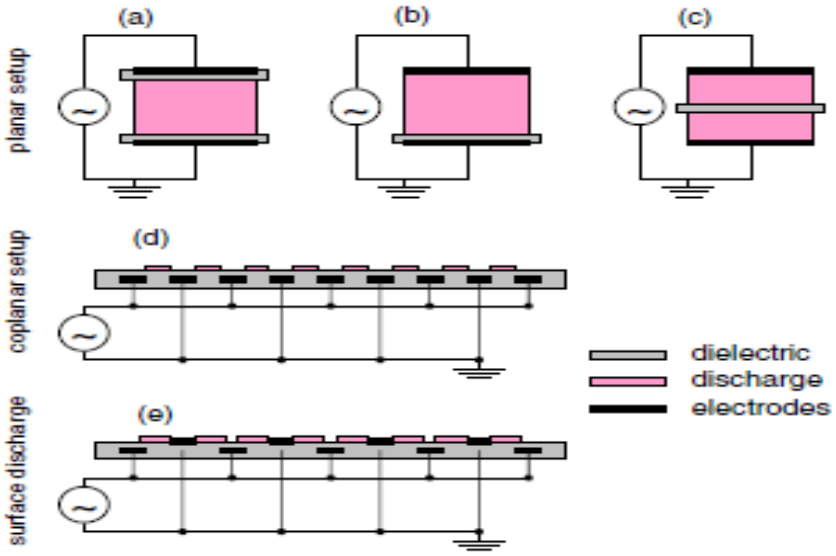

Figure 2: Illustration of CAPP generation using DBD (Ehlbeck et al., 2011; Wagner et al., 2003)

Atmospheric pressure plasma jet (APPJ):

APPJ is typically generated in a nozzle and comes out in the form of a jet. Plasma jets are usually non-thermal capacitively coupled plasma sources which operate at microwave/radio/even lower frequencies and consist of two electrodes in different arrangements (Ehlbeck et al., 2011). The mechanism of plasma generation is quite simple as there is a gas flow and a voltage gradient is applied between the electrodes leading to generation of plasma and the high flow rate of gas pushes the plasma out through the orifice in the form of a jet. The focused treatment area of the plasma jet can be an advantage or a disadvantage based on the application. Figure 3 illustrates some of the designs used for CAPP generation using APPJ. CAPP used in this research study was a plasma jet of arrangement “d”. (Figure 3)

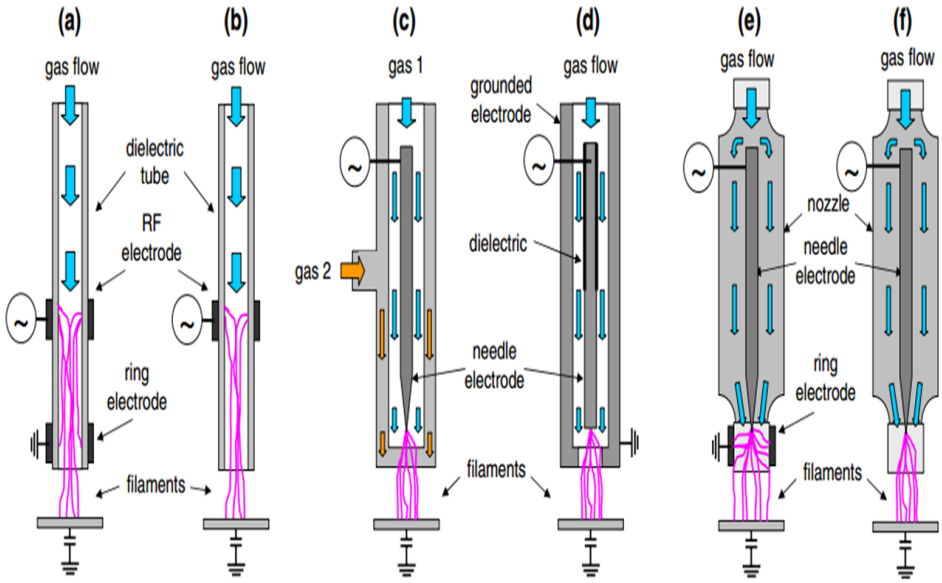

Figure 3: Illustration of different atmospheric pressure plasma jet setups based on electrode arrangements and gas inlets (Ehlbeck et al., 2011)

Corona discharge:

Corona discharge plasma is generated by application of high voltage near the electrode tip which leads to formation of plasma at the tip. Thus, ionization and luminosity are usually found at the electrode tips. A schematic of plasma generation via corona discharge is illustrated in Figure 4.

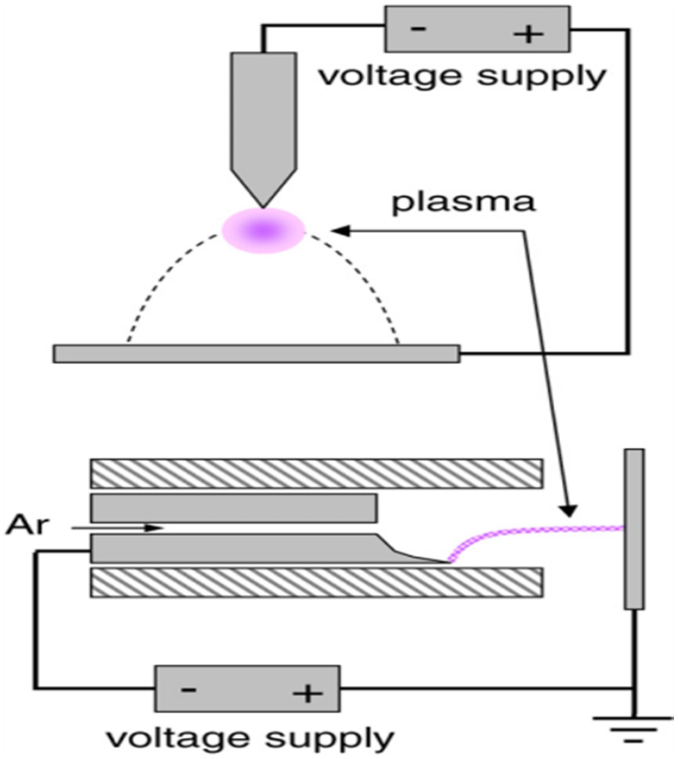

Figure 4: Illustration of CAPP generation via Corona discharge (Bussiahn et al., 2010; Ehlbeck et al., 2011; Scholtz et al., 2010)

Microwave driven plasma:

Microwave driven plasmas are generated without electrodes. Electrons absorb microwaves, gain kinetic energy and collide with heavy particles ionizing them and

generating plasma. Figure 5 illustrates a few designs in which plasmas can be generated using microwaves. A major advantage of microwave generated plasma is that it is electrodeless which makes it torch like and easy to handle.

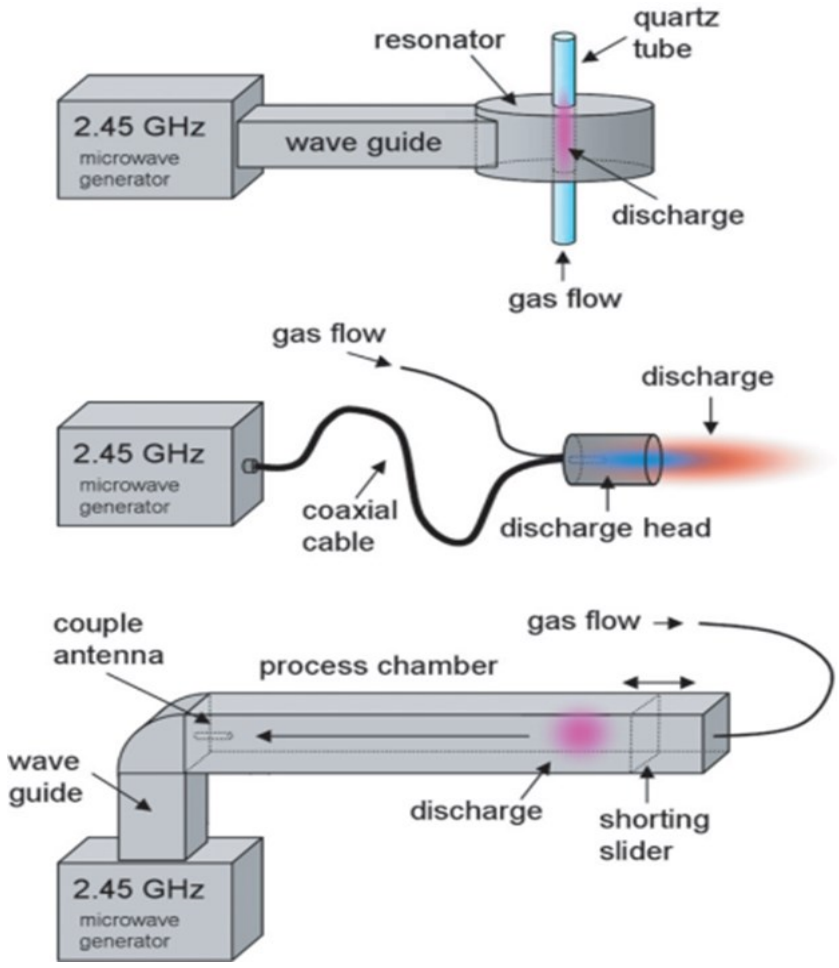

Figure 5: Illustration of CAPP generation using microwaves (Ehlbeck et al., 2011)

Table 2 shows a comparison of process parameters of the different plasma generation methods

Table 2: Illustration of parameter ranges for different plasma generation methods

Parameter	Corona Discharge	Dielectric Barrier Discharge	Atmospheric Pressure Plasma Jet	Microwave Driven Plasma
Temperature (K)	~300	~300	300-430	300-4000
Voltage (kV)	1-14	1.5-10.4	1-5	
Frequency	DC, pulsed DC	2 kHz - 21.7 kHz	1 kHz - 27.12 MHz	Typ. 2.45 GHz
Power (W)	50	1.8 – 360	15-250	85-1700
Flow rate (slm)	0-0.5	0-1.7	8-92	1-23.5
Used gases	Ar/air	Ar/air/humidity	He/Ar/O2/Air	Ar/air/humidity

Ehlbeck et al., 2011

1.1.2 CAPP Applications

CAPP is being used for various purposes in many industries due to its unique properties. Some of its major applications are:

<u>Auto industry:</u>

Car panels are treated with CAPP which increases their surface energy and enhances adhesion of paints and coating. The mechanisms which cause this surface

activation/increase of surface energy could be ablation, cross linking or surface activation based on the material being treated and the gas used (Carrino et al., 2002).

Ablation: When a substrate is treated with plasma, plasma particles bombard the surface and remove both molecular layers and organic residues from the surface. This causes an increase in the surface roughness of the substrate, which leads to increased number of links between the substrate and the coating.

Cross linking: When a substrate is treated with plasma, the bombardment of plasma particles causes a breakage of polymeric macromolecules and subsequently an increase in the sites for adhesion of coating onto the substrate.

Surface activation: Plasma oxidizes the surface and increases the polar groups which are directly related to the adhesiveness of the substrate.

Biomedical industry:

CAPP is used for cold sterilization of medical instruments and prostheses (Thirumdas et al., 2015). The mechanism of sterilization is inactivation of micro-organisms primarily via oxidation of cell constituents and electrostatic disruption which is explained in Section 1.1.3.

Wound healing:

CAPP has shown potential application for wound healing purposes due its efficiency in inactivating micro-organisms and enhancing the healing processes by enabling selective antimicrobial activity and via tissue regeneration (Isbary et al., 2013; Weltmann Klaus et al., 2010).

Food industry:

A great deal of research has been done in the last decade to evaluate the potential application of CAPP in the food industry, specifically for food decontamination purposes. Past research has shown CAPP as a potential surface decontamination technique on many substrates like fresh produce, meats, eggs, juices, etc., by achieving multi-log reductions of microbes like *Escherichia coli*, *Salmonella*, and *Listeria* (Fernandez et al., 2013; Lacombe et al., 2015; Lee et al., 2011; Misra et al., 2014; Ragni et al., 2010; Rød et al., 2012). CAPP has also shown the potential to inactivate spores and biofilms which are generally very difficult to inactivate (Abramzon et al., 2006; Niemira, 2012; Patil et al., 2014; van Bokhorst-van de Veen et al., 2015). Table 3 illustrates some of the microbial inactivation results from foods using CAPP.

Table 3: Illustration of microbial inactivation results on foods using CAPP

Substrate	Microorganism	Plasma Generation Method	Exposure Time	Feed Gas	Log Reduction	Reference
Chicken skin	*Listeria innocua*	Plasma Pen	8 min	He-O_2	0.77 ± 0.25 log CFU/cm2	(Noriega et al., 2011)
Chicken muscle	*Listeria innocua*	Plasma Pen	4 min	He-O_2	2.71 ± 0.54 log CFU/cm2	
Chicken breast	*Listeria monocytogenes*	Plasma Jet	2 min	N_2 + O_2	4.73 log CFU/g	(Lee et al., 2011)
Ham	*Listeria monocytogenes*	Plasma Jet	2 min	N_2 + O_2	6.72 log CFU/g	
Lettuce	*Salmonella* Typhimurium	Plasma Jet	15 min	N_2	2.72 ± 0.31 log CFU/sample	(Fernández et al., 2013)
Potato	*Salmonella* Typhimurium	Plasma Jet	15 min	N_2	0.94 ±0.30 log CFU/sample	
Strawberry	*Salmonella* Typhimurium	Plasma Jet	15 min	N_2	1.76 ± 0.67 log CFU/sample	
Strawberries	Yeast/molds	Dielectric Barrier Discharge	5 min	Air	2 log CFU/g	(Misra et al., 2014)
Golden delicious apples	*Escherichia coli* O157:H7	Gliding Arc	3 min	Air	3.6 log CFU/ml	(Niemira and Sites, 2008)
Tomatoes	*Listeria monocytogenes*	Dielectric Barrier Discharge	60 s + 24 hours	Air	5.1 ± 0.5 log CFU/sample	(Ziuzina et al., 2014)
Apple juice	*Escherichia coli* O157:H7	Needle/plate system	40 s		5 log CFU	(Montenegro et al., 2002)
Orange juice	*Staphylococcus aureus, Escherichia coli, Candida albicans*	Dielectric Barrier Discharge	25 s	Air	>5 log CFU/ml	(Xing-Min et al., 2011)
Almonds	*Escherichia coli*	Dielectric discharge	30 s	Air	1.8–5 log CFU/g	(Deng et al., 2007)
Hazelnuts, peanuts, pistachio nuts	*Aspergillus parasiticus*	Low pressure plasma	10 min	SF_6	5 log CFU/g	(Basaran et al., 2008)
Red pepper powder	*Aspergillus flavus* spores	Microwave driven	20 min	N2	2.5 ± 0.3 log	(Kim et al., 2014)

		plasma			spores/g	
GSWP filters	*Bacillus cereus* spores	Plasma Jet	20 min	N_2	3.7 ± 0.87 log	(van Bokhorst-van de Veen et al., 2015)
Bell peppers	*Pantoea agglomerans* biofilm	Dielectric Barrier Discharge	10 min	He-O_2	2 log CFU	(Vleugels et al., 2005)

CAPP is still not yet approved for use in food industry by the US FDA but as evident from Table 3, it has significant potential for decontamination of foods. CAPP has not always shown consistent results with respect to its effect on the quality attributes of treated commodities (Schluter et al., 2013). CAPP did show promising results on some of the commodities like cherry tomatoes where it did not adversely affect critical quality parameters of color, firmness, pH and weight loss (Misra et al., 2014). CAPP treatment resulted in increased flavonoid (luteolin and diosmetin) content on lamb's lettuce and on apple slices it inhibited enzymatic browning and reduced polyphenol oxidase activity (Grzegorzewski et al., 2010; Tappi et al., 2014). The advantage of using CAPP is that the food substrate can be treated at temperatures less than 50 °C and it is chemical and water free (Fernández et al., 2013; Fernández and Thompson, 2012; Kim et al., 2014; Scholtz et al.).

1.1.3 Mechanism of microbial inactivation

There is a great deal of speculation over the mechanisms by which CAPP inactivates microorganisms due to its complex and dynamic nature. However, two proposed

mechanisms of inactivation are via electrostatic disruption, and oxidation of cell constituents (Gaunt et al., 2006).

Electrostatic disruption:

In electrostatic disruption, the charged species generated in the plasma start accumulating on the bacterial cell membrane and eventually, the electrostatic force exceeds the tensile force of cell membrane leading to cell rupture. The tensile force is conferred by murein layer which is thicker in Gram-positive bacteria (~15 nm - 80 nm) than Gram-negative bacteria (~2 nm) which would lead to faster lysis of Gram-negative bacteria by CAPP than Gram-positive (Gaunt et al., 2006; Mendis et al., 2000). Figure 6 illustrates electrostatic disruption of an *Escherichia coli* cell after CAPP treatment. The Figure 6 (a) to the left shows a control untreated *E. coli* cell and the Figure 6 (b) to the right shows a CAPP treated *E. coli* cell with high degree of electroporation.

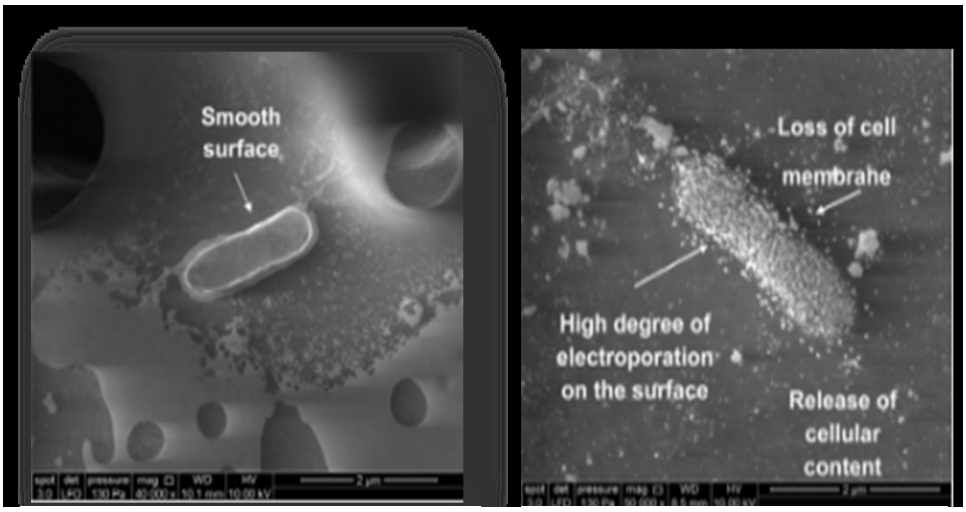

a) Control *E.coli* cell before plasma treatment

b) CAPP treated *E.coli* cell showing high degree of electroporation

Figure 6: Illustration of electrostatic disruption of an *Escherichia coli* cell after CAPP treatment (Bermúdez-Aguirre et al., 2013)

Oxidation of cell constituents:

In oxidation of cell constituents, the microbial inactivation is attributed to reactive oxygen and nitrogen species such as superoxide (O_2^-), hydrogen peroxide (H_2O_2), hydroxyl radicals (OH.), ozone (O_3), nitric oxide (NO), etc. These reactive species interact with cellular macromolecules like lipids, proteins, and DNA compromising their functionality and leading to cell death (Gaunt et al., 2006; Perni et al., 2007).

The reactive oxidative species interact with lipids in the cell membrane to start a process called lipid peroxidation as explained below (Gaunt et al., 2006).

Step 1 – Radicals (ex: $OH^{\cdot}$) abstract hydrogen from the side chain of an unsaturated fatty acid (L) to produce a carbon centered lipid radical ($L^{\cdot}$) and water

$$L + OH^{\cdot} \longrightarrow L^{\cdot} + H_2O$$

Step 2 – Lipid radical reacts with molecular oxygen to form a lipid peroxyl radical ($L\text{-}OO^{\cdot}$)

$$L^{\cdot} + O_2 \longrightarrow L\text{-}OO^{\cdot}$$

Step 3 – Lipid peroxyl radicals abstract hydrogen from the side chain of an unsaturated fatty acid forming another lipid radical and lipid hydro peroxide (L-OOH)

$$L\text{-}OO^{\cdot} + L \longrightarrow L^{\cdot} + L\text{-}OOH$$

Step 4 – Lipid hydro peroxides will give rise to lipid alkoxy radical via the Fenton reaction and short chain aldehydes via fragmentation

$$L\text{-}OOH \longrightarrow L\text{-}O^{\cdot}$$

Lipid peroxidation generates products which are shorter than the initial unsaturated fatty acids which results in their inability to rotate within the cell membrane. This compromises the structural integrity of the membrane leading to subsequent cell lysis.

Plasma reactive species interact with cellular proteins leading to changes like peptide fragmentation, protein-protein crosslinking, modification of amino acids side chains, reduction of disulphides, etc., which compromises their functionality and leads to cell lysis (Cabiscol et al., 2000).

Plasma reactive species cause DNA lesions through reactions with bases and sugar moieties. Intermediate intracellular radicals generated during lipid peroxidation can also react with DNA compromising its functionality and leading to cell lysis (Gaunt et al., 2006).

Table 4 illustrates the typical densities of plasma active species such as oxygen ions, oxygen atoms, ozone, and other charged species in different plasma discharges.

Table 4: Typical densities of oxygen ions, oxygen atoms, ozone, and charged species in different plasma discharges.

Source	Typical Density (cm^{-3})			
	O^+, $O_2.^+$, $O_2.^-$	O	O_3	Charged Species in Plasma
Low pressure Discharge	10^{10}	10^{14}	$<10^{10}$	10^8 - 10^{13}
Arc or Plasma jet	10^{15}	10^{18}	$<10^{10}$	10^{16} - 10^{19}
Corona	10^{10}	10^{12}	10^{18}	10^9 - 10^{13}
Dielectric Barrier Discharge	10^{10}	10^{12}	10^{18}	10^{12} - 10^{15}

(Loeb and Meek, 1940)

1.1.4 Parameters affecting microbial inactivation

The microbial inactivation efficacy of CAPP is affected by both process parameters and external factors. The process parameters include gas composition, treatment time, distance from plasma, etc. The external factors include substrate surface topography, initial microbial load on the substrate, type of bacteria, moisture content in the system, etc.

Process parameters:

Higher CAPP treatment times and system voltages have been associated with higher microbial inactivation on substrates (Deng et al., 2007; Joshi et al., 2011). Past research studies have used different feed gases such as helium, argon, nitrogen, air, carbon dioxide, etc. but it has been shown that feed gas having oxygen leads to a higher microbial inactivation due to generation of reactive oxygen species (ROS) like hydrogen peroxide, singlet and atomic oxygen which play the most crucial role in the inactivation of microbes (Dobrynin et al., 2009; Joshi et al., 2011; Kim et al., 2011; Moisan et al., 2001). The distance from the CAPP generator also plays a role as a greater distance from the CAPP emitter means the loss of charged particles and short lived antimicrobial species which would cease to exist by the time they reach the substrate, affecting the microbial inactivation (Fridman et al., 2007).

External factors:

Past research has shown that the microbial inactivation efficacy of CAPP depends to a large extent on the surface roughness of the substrate and the efficacy increases as the roughness decreases (Bermúdez-Aguirre et al., 2013; Fernandez et al., 2013; Noriega et al., 2011). It has been shown that bacteria attach themselves to complex surface features on rougher surfaces and escape plasma treatment, thus a lower microbial inactivation is achieved on rougher surfaces.

Previous research studies have shown that a higher initial microbial concentration on substrates reduces the microbial inactivation efficacy of CAPP (Deng et al., 2005; Fernández et al., 2012). Fernandez et al. reported an increase in D value from 0.20 ± 0.03 minutes to 2.81 ± 0.24 minutes as the initial cell concentration of *Salmonella* Typhimurium on membrane filters went up from 10^5 CFU/filter to 10^8 CFU/filter. This can be attributed to the fact that at higher concentrations, bacterial cells may be arranged in multilayers and the top layer of inactivated bacteria may work as a protective layer against plasma species for the lower layers.

A clear consensus has not been reached on susceptibility of Gram-positive and Gram-negative bacteria for CAPP treatment. Some studies report that Gram-positive bacteria are more resistant to CAPP treatments than Gram-negative bacteria (Ermolaeva et al.,

2011; Lee et al., 2006; Ziuzina et al., 2014). The rationale here is that microbial inactivation via electrostatic disruption where the tensile force is conferred by murein layer which is greater in Gram-positive bacteria which have a thicker layer (~15 nm - 80 nm) than Gram-negative bacteria (~2 nm) (Gaunt et al., 2006; Mendis et al., 2000). Other studies have revealed greater sensitivity of Gram-positive bacteria than Gram-negative bacteria (Fan et al., 2012). One possible explanation of this could be the thick lipolysacharide outer membrane of Gram-negative bacteria is a better shield to reactive plasma species than the thinner peptidoglycans membrane of Gram-positive bacteria (Tipa et al., 2012).

Past research has shown that presence of moisture on the substrate or in the system can cause a difference in the microbial inactivation of CAPP and that higher inactivation is achieved with higher moisture content in the system (Dobrynin et al., 2009; Dobrynin et al., 2011). This is attributed to greater generation of OH radicals which are strong antimicrobial species.

1.2. Surface roughness

Surface roughness is a component of surface topography and is defined as “the deviation in the direction of the normal vector of a real surface from its ideal form” (ESI,

2015). Figure 7 is a pictorial representation of various terms used to describe the surface topography of a substrate.

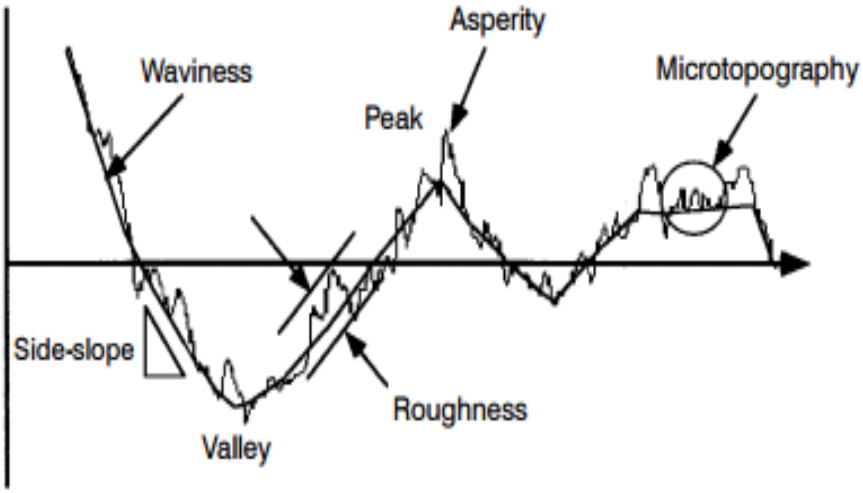

Figure 7: Terminology used to describe surface topography (Dove et al., 1996)

The topography of surfaces is comprised of superimposed waves of various wavelengths. The term “waviness” is used to designate long wavelength, high amplitude base-line undulations on which a series of short wavelength, lower amplitude irregularities are superimposed. The short wavelength irregularities constitute surface roughness. Micro topography refers to superimposed profiles at a localized region of the surface and become a part of surface roughness calculations on micro and nano level calculations. Describing surface roughness involves measurement of asperity height and distribution, asperity being the irregularities with respect to the base line. (Dove et al., 1996).

Surface roughness can be calculated based on three types of profiles (Jenoptik, 2008; ISO, 1997; Suelí Fischer Beckert, 2012).

P-profile is the primary profile which is a representative of the real surface and is obtained by filtering waves below a defined low pass wavelength. Primary profile is the basis for evaluation of primary profile parameters or P-parameters. The low pass wavelength is not fixed and is typically defined by the user.

R-profile is the roughness profile obtained from the primary profile by filtering longer waves (waviness components) as specified by a cutoff wavelength. Roughness profile is the basis for evaluation of roughness profile parameter or R-parameters. The cutoff wavelength is not fixed and is typically defined by the user.

W-profile is the waviness profile which is obtained from the primary profile by filtering shorter waves (roughness components) as specified by cutoff wavelength

Figure 8 illustrates the differences in the three types of profiles

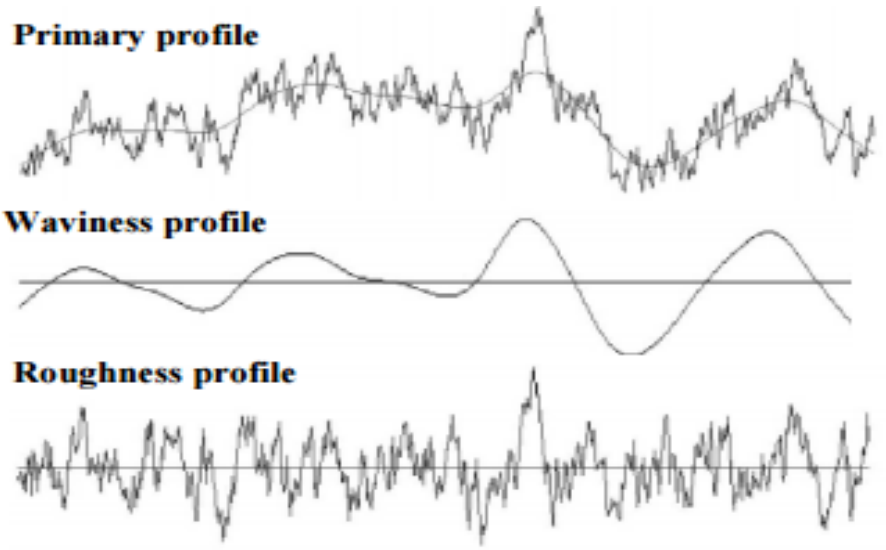

Figure 8: Surface roughness measurement profiles (Corporation, 2009; Jenoptik, 2008; Standardization, 1997; Suelí Fischer Beckert, 2012)

Two of the most widely used parameters used to quantify roughness are arithmetical mean deviation of assessed profile and root mean square deviation of assessed profile.

Arithmetical mean square deviation of assessed profile is represented by Pa/Ra/Wa based on the profile being used for calculation

$$\text{Pa/Ra/Wa} = \left(\frac{1}{l}\right) * \int_0^l |z(x)| dx \qquad \text{(Equation 1)}$$

where l = lp, lr, lw based on the profile being evaluated, z is peak or valley height at every point (x) along the length l

Root mean square deviation of assessed profile is represented by Pq/Rq/Wq based on the profile being used for calculation

$$Pq/Rq/Wq = \sqrt{\left(\frac{1}{l}\right) * \int_0^l z^2(x)dx} \quad \text{(Equation 2)}$$

where l = lp, lr, lw based on the profile being evaluated, z is peak or valley height at every point (x) along the length l.

Pa/Ra/Wa are the parameters most commonly used to characterize surface roughness due to ease of measurement. They are not typically used in scientific studies as they are less sensitive than Pq/Rq/Wq. Pq/Rq/Wq are more sensitive to asperity distributions as the amplitudes are squared and are typically used in scientific studies (BCM, 2010).

1.2.1. Effect of surface roughness on microbial inactivation efficacy of decontamination treatments:

Past research has shown that as the surface roughness of substrate increases, the microbial inactivation efficacy of decontamination technique decreases. Wang et al. (2009) checked the efficacy of acidic electrolyzed water, peroxyacetic acid, and sterilized deionized water for washing apples, oranges, avocados, and cantaloupes inoculated with a cocktail of five *Escherichia coli* O157:H7 strains and found that cantaloupe which had the roughest surface had the highest residual bacterial population post washing (Wang et al., 2009). Ringus and Moraru (2013) checked the efficacy of pulsed light treatment on food packaging materials like low density polyethylene (LDPE), high density polyethylene (HDPE), polyethylene-laminated ultra-metalized polyethylene

terephthalate (MET), polyethylene-coated paperboard (TR), and polyethylene-coated aluminum foil paperboard laminate (EP) inoculated with *Listeria innocua* and found higher surface roughness resulting in lower microbial inactivation (Ringus and Moraru, 2013). Research studies have also shown that the microbial inactivation efficacy of CAPP on substrates like fresh produce and chicken skin depends to a large extent on surface roughness, and the efficacy increases as the roughness decreases (Bermúdez-Aguirre et al., 2013; Fernandez et al., 2013; Noriega et al., 2011). The reason behind the observed inactivation trend is thought to be that bacteria attach themselves to complex surface features on rougher surfaces and escape decontamination treatment, thus a lesser microbial inactivation is seen on rougher surfaces.

Figure 9 illustrates surface structures and *Salmonella* Typhimurium inoculated on a membrane filter, a lettuce surface, a strawberry surface, and a potato tissue surface. The figure clearly illustrates the complex topography of the surface of lettuce, strawberry and potato surfaces, and the bacterial attachment sites on the surfaces (indicated by red circles) through which they escape decontamination.

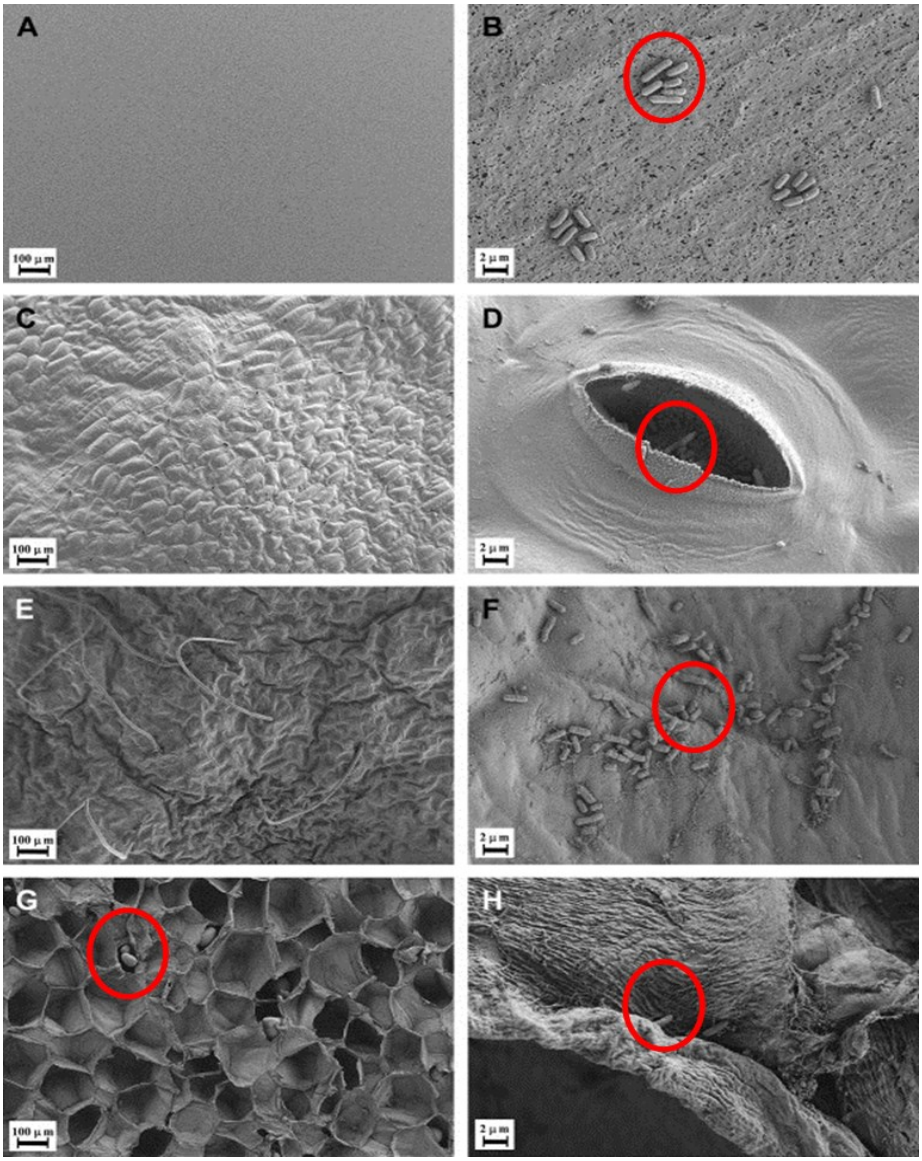

Scanning electron micrographs of inoculated substrates: A) & B) membrane filters (250× and 10,000×, respectively); C) & D) lettuce (250× and 10,000×, respectively); E) & F) strawberry (250× and 10,000×, respectively): G) & H) potato (250× and 10,000×, respectively).

Figure 9: Illustration of surface structures and *Salmonella* Typhimurium inoculated on a membrane filter, lettuce surface, strawberry surface, and potato tissue surface (Fernández et al., 2013)

1.3. Sandpapers

Note: All the information on sandpapers is adapted from (Klingspor Abrasives, 2015).

Sandpaper is a paper with an adhered abrasive material. It is commonly used in smoothing or polishing woodwork or other surfaces. Sandpaper essentially consists of three components – abrasive grains, glue, and backing. Sandpapers can be of many types based on the variations in above three components.

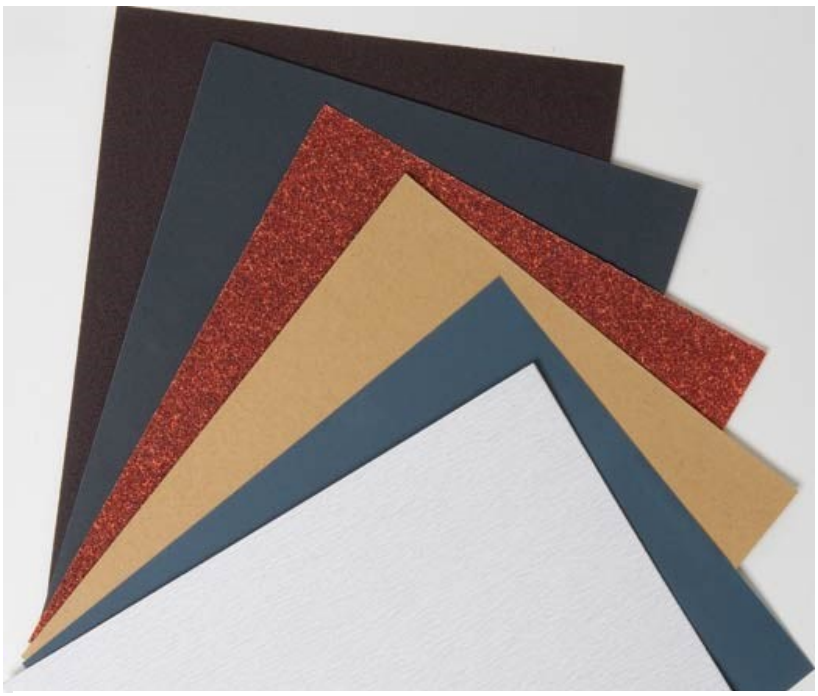

Figure 10: Illustration of different sandpapers available in the market (WorthPoint, 2010)

Abrasive:

There are four common materials for abrasive grains – aluminum oxide, silicon carbide, alumina zirconia, and ceramics. Aluminum oxide is known for its toughness and durability and is typically used for sanding steel, wood, and other tough materials. Silicon carbide grains are extremely sharp yet brittle. So, sandpapers with silicon carbide are used when a more consistent finishing on a material is required and pressure required is lower. Alumina zirconia is a superior grain and sandpapers with these grains are typically 20% - 40% more expensive than the others. It is used in applications where time and fast removal rates are the prime factors. Ceramic grains are usually used when rough grinding on metals is required. These grains can cover entire surface of the backing or just part of the backing and are classified into closed coat or open coat based on it. In closed coat sandpapers, 100% of the backing is covered with grains. In open coat sandpapers, only 50% - 70% of the backing is covered with grains. Closed coat sandpapers have a uniform topography and are usually preferred in most of the sanding application as they provide uniform sanding.

Sandpapers are also classified into different grits. Several different standards have been set for grit sizes but one of the most common ones is by United States CAMI (Coated Abrasive Manufacturers Institute, now part of the Unified Abrasives Manufacturers' Association).

Table 5: CAMI classification of sandpapers into grits

Type		CAMI Grit Designation	Average particle diameter (µm)
Macro grits	Extra coarse	24	708
		30	632
		36	530
	Coarse	40	425
		50	348
	Medium	60	265
		80	190
	Fine	100	140
		120	115
	Very Fine	150	92
		180	82
		220	68
Micro grits	Very Fine	240	53
	Extra Fine	320	36
		360	28
	Super Fine	400	23
		500	20
		600	16
	Ultra Fine	800	12.6

		1000	10.3

(SeaBeans, accessed on 05/11/2015)

Backing:

The backing for the sandpaper can be made of paper, cloth, or fiber depending on the usage. Paper backings are available in different thicknesses from “A” (lightest weight) to “F” (heaviest weight). Paper backings are not usually waterproof but can be chemically treated to make them waterproof. Cloth backings are classified into J, X, and Y types. J and X types are made up of cotton while Y is made of 100% polyester. Fiber backings are a combination of stacks of paper backings to make a very strong and durable paper backing.

Bonding:

Each sandpaper has two layers of adhesive bonding. The first layer, referred to as the maker coat, is what adheres the grain to the backing. The second layer, referred to as the size coat, ties the individual grains together (so that they act as a unit as opposed to acting as individual grains) and provides protection against heat. Sandpapers can be either resin bonded or glue bonded based on the manufacturer and usage. The glue bonded sandpapers are used in applications where a softer finish is required whereas resin bonded sandpapers are used when sharp cuts and product life are important factors.

Closed coat sandpapers of three different grits were used in this research study for their uniform and quantifiable surface topography, to isolate and investigate the effect of surface roughness on microbial inactivation efficacy of CAPP. More details will be given in later sections.

1.4. Fresh produce

Produce is a generalized term used to describe agricultural products and especially fresh fruits and vegetables as distinguished from grain and other staple crops (Merriam-Webster, accessed on 05/11/2015). In recent years, consumers demand for nutritious, safe, and minimally processed foods has promoted increased consumption of commodities such as fresh produce (Perni et al., 2008). According to Palumbo et al. (2007), fresh cut fruit and vegetable sales have grown to approximately $15 billion per year in the North American foodservice and retail market and account for nearly 15% of all produce sales. The largest portion of US fresh-cut produce sales at retail are fresh-cut salads, with sales of $2.7 billion per annum (Mary S. Palumbo, 2007). This trend has also been associated with an increase in the number of food borne outbreaks related to fresh produce (FAO/WHO, 2008). Table 6 lists selected US multistate foodborne outbreaks due to fresh produce in the last five years (CDC, 2015).

Table 6: List of selected multistate foodborne outbreaks due to fresh produce in the last five years

Year	Commodity	Pathogen	Number of states affected	Number of patients
2014	Cucumbers	*Salmonella* Newport	29	279
	Commercially Produced, Prepackaged Caramel Apples	*Listeria monocytogenes*	12	35
	Bean Sprouts	*Salmonella* Enteritidis	12	115
	Cilantro	*Cyclospora*		304
	Raw Clover Sprouts	*Escherichia coli* O121	6	19
2013	Ready to eat salads	*Escherichia coli* O157:H7	4	33
	Fresh produce	*Cyclospora cayetanensis*	25	631
	Cucumbers	*Salmonella* Saintpaul	18	84
2012	Spinach and spring mix	*Escherichia col*i O157:H7	5	33
	Mangoes	*Salmonella* Braenderup	15	127
	Cantaloupe	*Salmonella* Typhimurium and *Salmonella* Newport	24	261
2011	Romaine Lettuce	*Escherichia coli* O157:H7	10	60
	Jensen Farm Cantaloupes	*Listeria monocytogenes*	28	147
	Whole fresh imported papayas	*Salmonella* Agona	25	106
	Del Monte Cantaloupes	*Salmonella* Panama	10	20
2010	Alfalfa sprouts	*Salmonella* serotype I 4,[5],12:i:-	26	140

	Alfalfa sprouts	*Salmonella* Newport	11	44
	Shredded Romaine Lettuce	*Escherichia coli* O145	5	26

US FDA's definition of fresh-cut fruits and vegetables or fresh-cut produce is "fresh fruits and vegetables for human consumption that have been minimally processed and altered in form by peeling, slicing, chopping, shredding, coring, or trimming, with or without washing, prior to being packaged for use by the consumer or a retail establishment (e.g., pre-cut, packaged, and ready-to-eat salad mixes)." (FDA, 2009). Also, the FDA states that "Fresh-cut produce does not require additional preparation, processing, or cooking before consumption, with the possible exception of washing or the addition of salad dressing, seasoning or other accompaniments." (FDA, 2009). Due to the minimal interventions for microbial reduction, fresh produce becomes susceptible to microbial contamination at various stages such as while growing in the field, during processing, packing or in the home/restaurant kitchen. Current industry post-harvest disinfection methods like washing with chlorinated water, chlorine dioxide, hydrogen peroxide, ozone, and other disinfecting agents are not effective, can leave residues, and possess a handling risk (Artés et al., 2009; Gil et al., 2009; Gil et al., 2015; Ölmez and Kretzschmar, 2009). Fresh produce also cannot be subjected to heat processing as that would compromise the "fresh" nature of the product.

Thus, alternative non-thermal food processing techniques such as CAPP should be studied for decontamination of fresh produce so that the produce remains fresh, retains its nutritional quality, and is microbiologically safe to consume.

1.5. Background on the instruments used in this research study

1.5.1 Scanning electron microscopy

Scanning Electron Microscopy (SEM) is a type of electron microscopy which produces an image of the sample by scanning it with a beam of electrons. SEM has become a powerful research tool for its high magnification power up to 300,000X times, and its ability to reveal topographical information and chemical composition of even a nanospace area of sample (AMMRF, 2014). The principle behind SEM is that a high energy beam of electrons is incident on the sample and upon impact, the electrons lose their energy and produce variety of signals through electron-sample interactions. These signals include secondary electrons, backscattered electrons, diffracted backscattered electrons, photons, x-rays, visible light, and heat. There is a detector to detect each of the signals and convert it to depict a certain aspect of the image. Some of the important signals include secondary electrons which depict the topography of the sample, backscattered electrons which illustrate contrasts in composition in multiphase samples, diffracted backscattered electrons which determine crystal structures and orientations of minerals, and x-rays which are used for elemental analysis. The specific capabilities of

a SEM instrument depend on what detectors it has (Geochemical Instrumentation and Analysis, 2013). Figure 11 illustrates the working of an SEM.

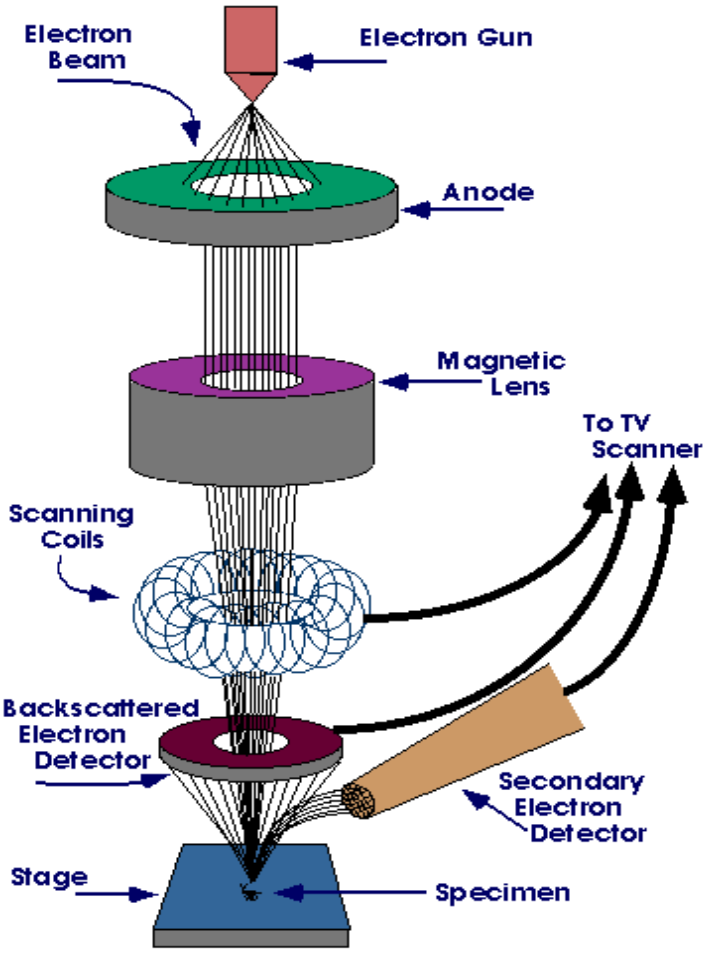

Figure 11: Illustration of working principle of SEM (Purdue, 2014)

The quality of a SEM image depends to a large extent on the sample preparation method. All samples being imaged must be electrically conductive/surface should be electrically conductive, and electrically grounded to prevent accumulation of electrostatic charge at the surface. Therefore, all samples are usually sputter coated

with an electrically conductive material like gold, gold/palladium alloy, osmium, etc., just prior to imaging. The specimen chamber is a high vacuum chamber, hence it is essential that sample is dry to prevent evaporation of water later. This adds three extra steps to sample preparation for biological samples. Biological samples need to be fixed and dried before sputter coating with an electrically conductive material. Fixation is done to prevent collapse of structures during imaging and is generally done using glutaraldehyde or osmium. The sample is then dehydrated by washing with ethanol or acetone which essentially replaces the water in the cells with the aforementioned chemicals. The next step is critical point drying (CPD) which is used to replace all of the ethanol/acetone with liquid carbon dioxide under pressure (this step is also done for wet non-biological samples) (University of Oklahoma, accessed on 05/11/2015)

Many research studies in the field of food science have used SEM to demonstrate surface topography of commodities like fresh produce, chicken skin, etc., and for bacterial attachment on these substrates as shown in Figure 9 (Bermúdez-Aguirre et al., 2013; Fernández et al., 2013). SEM was used in our research for the same purpose of viewing surface topography and bacterial attachment to the substrate.

1.5.2 Confocal laser scanning microscopy

Confocal Laser Scanning Microscopy (CLSM) is a technique used to obtain high resolution optical images with depth selectivity, through a process called optical sectioning. A conventional microscope "sees" as far into the specimen as the light can penetrate, while a confocal microscope only "sees" images one depth level at a time. (Vesely, 2007). This allows for images to be captured at various depths so as to reconstruct a 3D image of the sample.

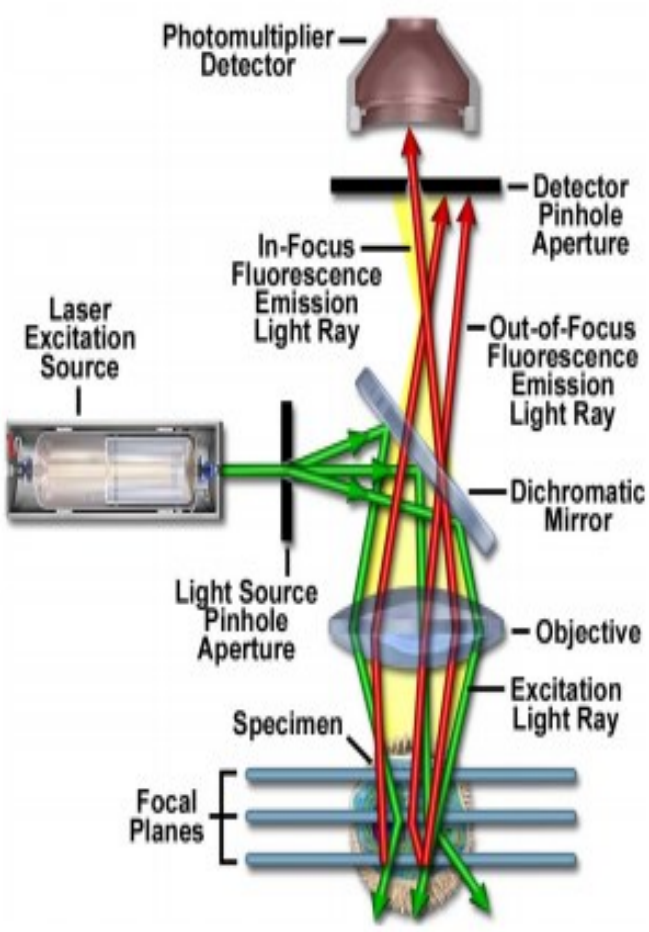

Figure 12: Illustration of the working principle of CLSM (Semwogerere, 2005)

The confocal microscope image is obtained either by reflecting light off the specimen or by stimulating fluorescence from dyes applied to the specimen. A laser of a specific wavelength is used to provide the excitation light (represented by green color in the Figure 12). This excitation light is reflected onto the sample using a dichromatic mirror and an objective. A dichromatic mirror is one which reflects light shorter than a certain wavelength and passes light longer than that wavelength. By adjusting equipment parameters and the objective, this light can be focused at different focal planes/different depths on the sample, thus allowing to scan and image one depth at a time. CLSM can be operated in regular reflection mode or fluorescence mode. Depending on the mode being used, the sample molecules upon being hit by a high energy light, will reflect the laser beam or fluoresce to emit light of different wavelength (red color in Figure 12). This light passes through the objective and the dichromatic mirror to the detector where the signal is converted into an image, one pixel at a time. These 2D images can be reconstructed into a 3D image to reveal information on the surface topography of an opaque sample or interior structures can be imaged for non-opaque samples (Prasad et al., 2007).

CLSM has been demonstrated to be an efficient tool in surface topography characterizations of complex geometries (Buajarern et al., 2014). Also, there is minimal sample preparation and it is a non-invasive/non-contact technique which is an advantage over contact surface characterization techniques like Atomic Force

Microscopy (AFM) as it can be used even on delicate substrates. CLSM has been used to characterize the surface topography of food substrates such as apples, avocadoes, cantaloupes, etc. (Sheen et al., 2008; Wang et al., 2009). In our study CLSM was used for measuring surface topography of sand papers and fruit surfaces.

1.5.3. Optical emission spectroscopy

Optical Emission Spectroscopy (OES) is an analytical technique which uses measurement of the optical emission from excited atoms to identify the analyte/reactive species generated by the analyte. OES works on the principle that when sufficient energy is supplied for the ionization of a substance, high energy species like atoms, ions and electrons are generated in the system. These high energy species are specific to the substance being ionized and upon loss of energy, they transition from a higher energy level to a lower energy level. These transitions liberate photons of characteristic wavelengths which are detected by the Optical Emission Spectrometer and recorded on the spectrum. Photons of different wavelengths can be detected simultaneously by OES and thus a spectrum of the element is generated. We can identify the substance based on this spectrum or if the composition of substance is known, we can identify the species that are being generated. Thus, OES can be used either to identify the analyte or reactive species generated by the analyte based on the spectra (Chemicool, 2014; Machala et al., 2007).

OES has been used as a tool for identifying and relatively quantifying the plasma species in the field of food science and particularly for cold plasma (Surowsky et al., 2014; van Bokhorst-van de Veen et al., 2015). We also used OES in this research study.

1.6. Rationale and research objectives

The past research studies showed that the microbial inactivation efficacy of CAPP depends to a large extent on the surface roughness of the substrate and the efficacy increases as the roughness decreases (Bermúdez-Aguirre et al., 2013; Fernández et al., 2013; Noriega et al., 2011). However, most of the studies on microbial inactivation efficacy of CAPP dealt with complex substrates like fresh produce, chicken skin, etc. where many other parameters could also play a role in microbial inactivation such as moisture content of the surfaces, presence and composition of natural and artificial waxes on the surfaces, migration of microorganisms from the exterior to the interior, surface energy of the substrates, etc. (Dobrynin et al., 2009; Dobrynin et al., 2011) have shown that presence of moisture on the substrate or in the system can cause a difference in the microbial inactivation by CAPP and that higher inactivation is achieved with higher moisture content in the system. Also, each fruit might have a different composition of natural waxes on its surface (Kolattukudy, 1984) which might affect the microbial inactivation efficacy of CAPP. For example, natural wax on apple is dominated by a compound called ursolic acid which is highly water repellant. This might reduce microbial attachment on the surface of an apple as leading to greater microbial

inactivation. Research studies have also reported that microbes such as *E. coli* and *S. cerevisiae* on surfaces can migrate towards the interior of the matrix escaping plasma treatment (Keeratipibul et al., 2011; Perni et al., 2008; Richards and Beuchat, 2005). Microbial inactivation can also be affected by the degree of bacterial adhesion to the substrate which depends on the surface energy of the substrate. The microbial adhesion could increase or decrease with increasing surface energy of substrates and that would depend on the physical and chemical properties of bacteria, substrates, and water solutions (Liu and Zhao, 2005). Previous research studies have shown that a higher initial microbial concentration on substrates reduces the microbial inactivation efficacy of CAPP (Fernández et al., 2012).

None of the research studies cited above focused on the isolated effect of surface roughness on the microbial inactivation efficacy of CAPP. Thus, it became of interest to check if surface roughness did play a role in microbial inactivation efficacy of CAPP and if yes, to what extent for fresh produce decontamination. Hence, the objectives of this research study were i) To isolate and investigate the effect of surface roughness on microbial inactivation efficacy of CAPP from air by using a model system (sandpapers). ii) To understand the extent to which surface roughness affects the microbial inactivation efficacy of CAPP from air on a fresh produce. iii) To detect and relatively quantify plasma species under a plasma jet from air.

Based on the above objectives, suitability of CAPP for fresh produce decontamination was determined.

2. MATERIALS AND METHODS

2.1 Materials

2.1.1. Bacterial culture

The bacterium used in this research was nalidixic acid resistant *Enterobacter aerogenes* B 199A (VivolacCultures, Indianapolis, Indiana, USA). This strain of *E. aerogenes* is reportedly non-pathogenic and possesses similar attachment characteristics as *Salmonella* spp. (Zhao et al., 1998). *Salmonella* has been associated with food borne disease outbreaks over the last few years including on fresh produce such as cucumbers, bean sprouts, mangoes, cantaloupes, etc. (CDC, 2015) (Table 6).

2.1.2 Media used for culturing *E. aerogenes*

Glycerol stock for long term storage of *E. aerogenes*: Eighty percent glycerol solution was prepared by mixing of 8 parts of glycerol and 2 parts of water. The mixture was then autoclaved at 121 °C for 15 minutes and allowed to cool. *E. aerogenes* was grown in Tyrptose Phosphate Broth (explained in section 2.2.3.) for 18 h at 37 °C. One half ml of this bacterial culture was added to 0.5 ml of the glycerol stock in a sterile screw cap micro centrifuge tube and stored at -80 °C for further use.

Nalidixic acid stock solution: Nalidixic acid stock solution was prepared in a 10 ml sterile centrifuge tube. Eight hundredths grams of sodium hydroxide (Fisher BioReagents, USA) was dissolved in 10 ml of distilled water in a centrifuge tube. One half gram of Nalidixic acid (Fisher BioReagents, USA) was added to it. The nalidixic acid concentration used in this research study was 50 µg/ml.

Tryptic soy agar: Difco Tryptic Soy Agar (Becton, Dickinson & Company, USA) was prepared by adding 40 g to 1 liter of distilled water. The solution was autoclaved at 121 °C for 15 minutes and allowed to cool down to 60 °C. Nalidixic acid was added to give a concentration of 50 µg/ml and poured into 20 ml sterile petri dishes.

Tryptose phosphate broth: Bacto Tryptose Phosphate Broth (Becton, Dickinson & Company, USA) was prepared by adding 2.95 g to 100 ml of distilled water. The solution was autoclaved at 121 °C for 15 minutes and allowed to cool down to 60 °C. Nalidixic acid was added to give a concentration of 50 µg/ml and was filled into sterile centrifuge tubes.

MacConkey agar: Baltimore Biological Laboratory (BBL^{TM}) MacConkey Agar (Becton, Dickinson & Company, USA) was prepared by adding 50 g of it to 1 liter of distilled water. The solution was autoclaved at 121 °C for 15 minutes and allowed to cool down

to 60 °C. Nalidixic acid was added to give a concentration of 50 µg/ml and poured into 20 ml sterile petri dishes.

One tenth percent peptone water: Peptone Water was prepared by dissolving 1.5 g of peptone powder (Becton, Dickinson & Company, USA) in 1 liter of distilled water. The solution was divided into 9 ml aliquots in glass tubes for serial dilution and 49 ml aliquots into 500 ml glass bottles. These were sterilized by autoclaving at 121°C for 15 minutes.

2.1.3. Sandpapers

In order to isolate the effect of surface roughness on microbial inactivation efficacy of CAPP, a model system was needed in which the only varying parameter was surface roughness. Sandpapers of different grits satisfied the above requirement along and had a uniform topography verified via Scanning Electron Microscopy. Sandpapers (Norton Brand manufactured by Saint-Gobain Abrasives Inc., Montgomeryville, PA) were purchased from local Grainger store. Three grits of close-coat waterproof sandpaper T414 used were: Grit 280, Grit 400, and Grit 600.

2.1.4. Fruits

Fruits were selected such that their surface roughness matched closely to the selected grits of sandpapers (Sheen et al., 2008; Wang et al., 2009). Golden Delicious Apples (Variety 4020), Sunkist Valencia Oranges (Variety 4388), and Cantaloupes (Variety 4050) were purchased from local supermarket and transported to the laboratory where they were held at 4 °C and used within 3 days.

2.1.5. CAPP equipment:

The CAPP equipment used for this research was purchased from Plasma Treat Inc. (Elgin, IL). The equipment consisted of the plasma generation device (FG5001) and a rotating nozzle (RD1004). Plasma was generated using OPENAIR^{TM} PLASMA JET TECHNOLOGY at a voltage of 295 V, air pressure of 1990 mBar, and frequency of 22.5 kHz. The feed gas for the plasma was dry (moisture free), filtered air. Plasma was generated in the discharge chamber by applying a voltage between inner and ring electrodes (Figure 13).

Figure 14 illustrates the CAPP equipment in our laboratory. Figure 15 shows a more focused depiction of the plasma nozzle and substrate being treated. An important point to note here is that the substrate is placed at a specific distance from the nozzle on a rotating plate and is rotated under the plasma jet at a specific rpm. Determination of the substrate distance from plasma nozzle will be explained below.

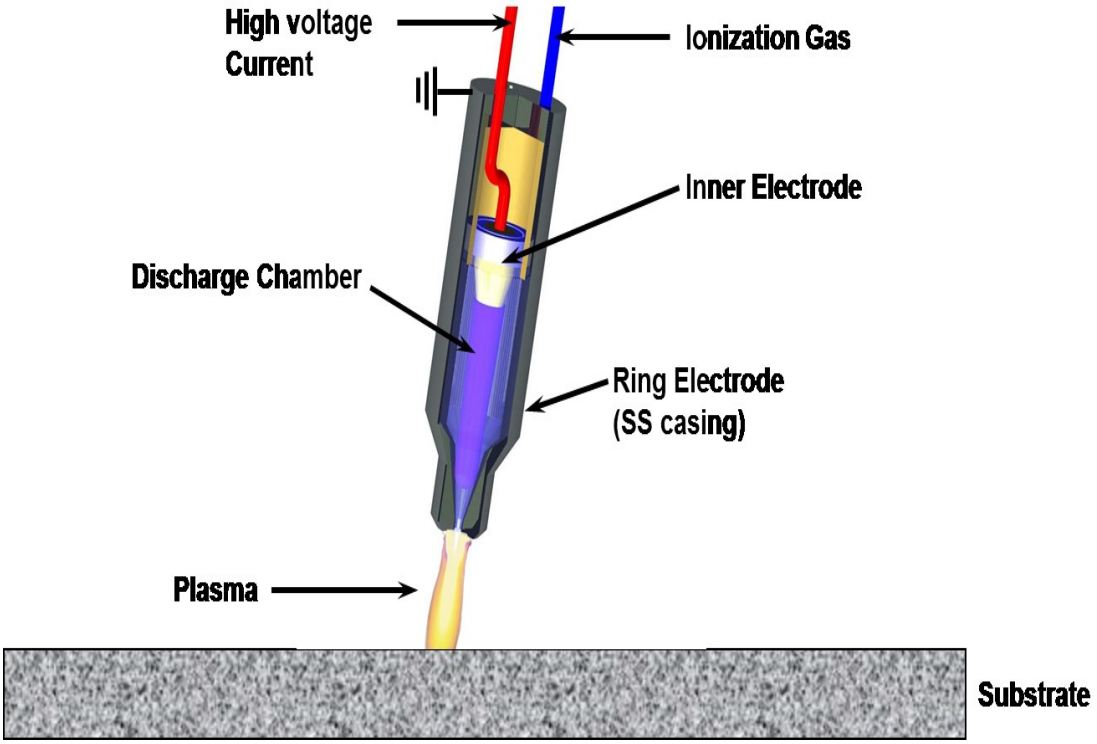

Figure 13: OPENAIR^{TM} PLASMA JET used in this research study (Plasma Treat Inc.)

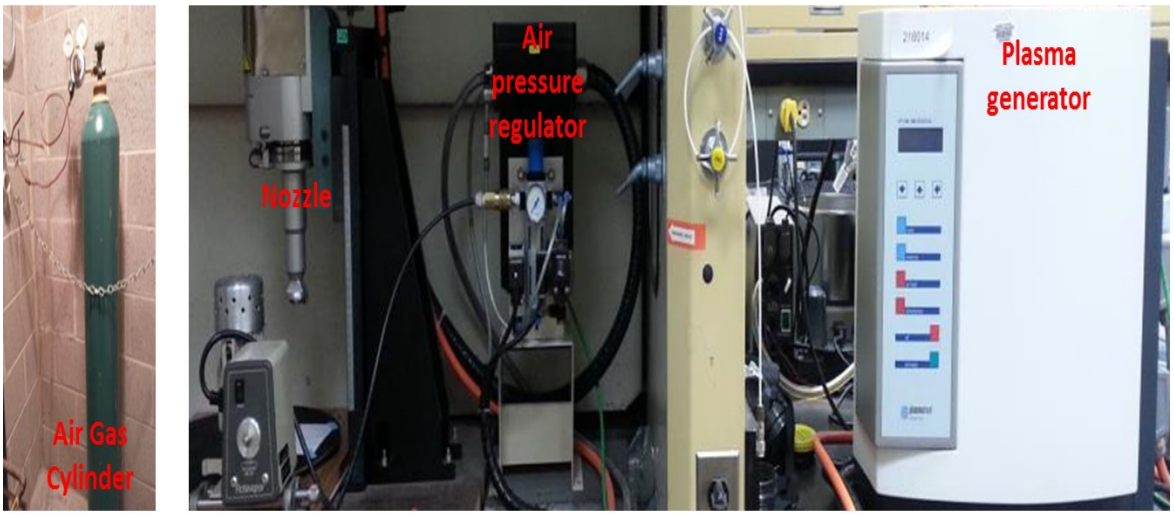

Figure 14: CAPP unit at Food Science Department, Rutgers University

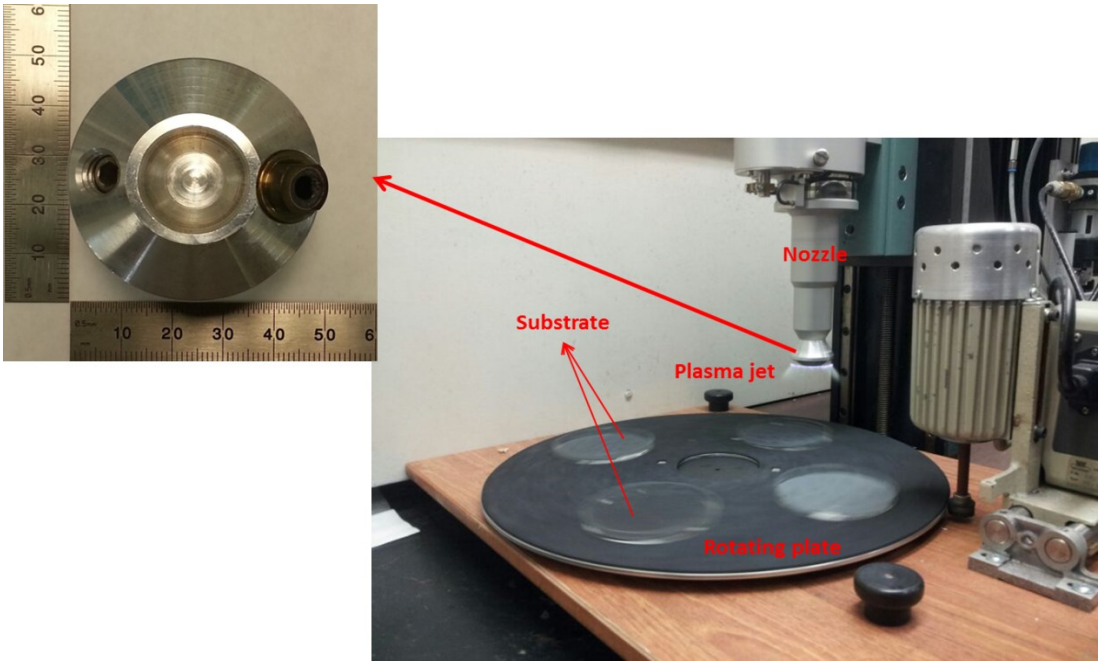

Figure 15: CAPP setup depicting plasma nozzle and substrates being treated under plasma jet

2.1.6. Instruments used in this research study

- ✓ Infrared camera (Model TI125-12110128, Fluke Inc., Everett, WA)
- ✓ Scanning Electron Microscope (Zeiss Sigma Field Emission SEM with Oxford EDS, Jena, Germany) located at Ceramic, Composite and Optical Materials Center, Rutgers University
- ✓ Leica TCS SPII Confocal Microscope (Buffalo Grove, IL) located at the Department of Biomedical Engineering, Rutgers University
- ✓ Black-Comet UV-VIS Spectrometer (StellarNet Inc., Tampa, USA) with a F400-UV–vis-SR fiber optic in the range from 190 nm to 850 nm and a collimating lens QCol.

2.2. Methods

2.2.1. Determining substrate distance from plasma nozzle

Although it is called cold atmospheric pressure plasma, the plasma is hot inside and near the jet nozzle. However, the plasma jet rapidly cools down within a short distance. Thus it was essential to determine a suitable distance to keep the substrate under the plasma where the microbial inactivation would be due to the effect of plasma only and not due to temperature.

First step was determining the maximum temperature which *E. aerogenes* can withstand without being inactivated. This led to performing preliminary experiments where *E. aerogenes* was exposed to different temperatures starting from 40 °C to 70 °C for various times from 1 minute to 7 minutes in a laboratory oven (Yamato ADP 31 Vacuum oven, Yamato Scientific America Inc. CA). Experimental protocol included growing a culture of *E. aerogenes* overnight as explained in section 2.2.5. The overnight culture was serially diluted and plated onto MacConkey agar. The MacConkey agar petri dishes were placed in the oven at varying temperatures, and for varying times. The petri dishes were then removed from the oven, incubated at 37 °C for 18 h, enumerated and compared against the inoculated untreated controls (inoculated MacConkey agar petri dishes which were not heated but were just incubated at 37 °C for 18 h). No inactivation was observed on subjecting *E. aerogenes* to as much as 65 °C for 7 minutes. It was decided to subject the bacteria to a maximum temperature of 50 °C to ensure that the bacterial inactivation would be due to plasma with no contribution of temperature.

An infrared camera was used to measure the temperature of the substrate at various distances from the plasma nozzle. It was determined that when the substrate (plane normal to the direction of plasma jet) was at a distance of ≥ 7.7 cm from the plasma nozzle the temperature was ≤ 50 °C (Figure 16). This was also confirmed using alcohol based thermometer. Thus, a substrate distance of 7.7 cm was used in this research study. A schematic of CAPP setup used in this research study is illustrated in Figure 17.

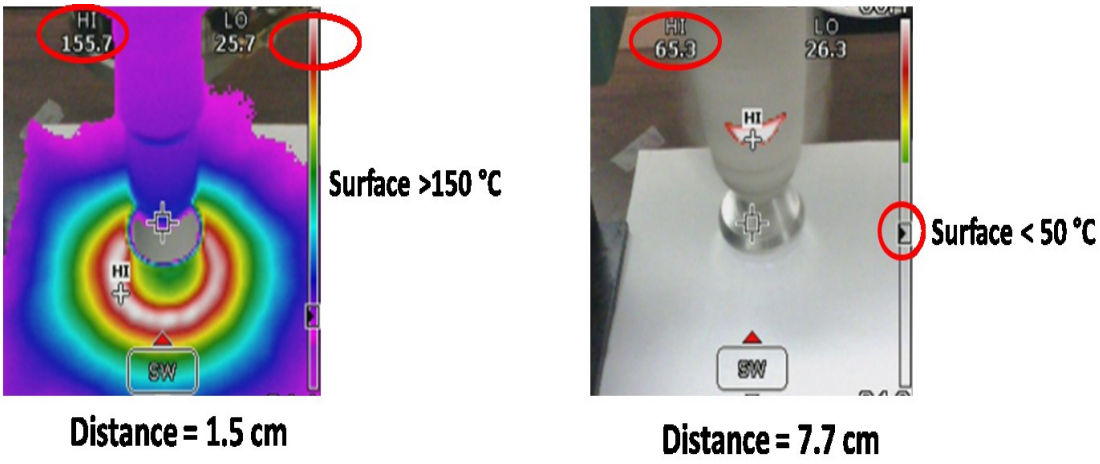

Figure 16: Infrared images when substrate was at a distance of 1.5 cm and 7.7 cm from the nozzle

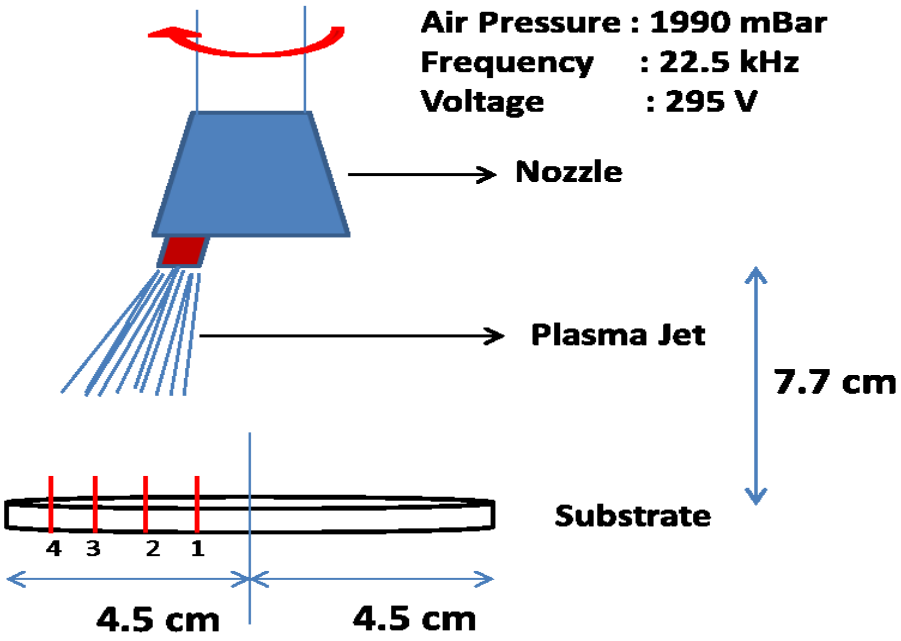

Figure 17: Schematic of CAPP setup used in this research study

2.2.2. Determining rotation time of substrate under plasma jet and CAPP treatment time

As explained in section 2.2.5., all bacterial inactivation experiments were performed by placing sandpapers/fruits in 9 cm diameter petri dishes. These petri dishes were kept on a plate which rotated under the plasma jet at a specific speed. Thus, for CAPP exposure treatment time of "x" minutes, the actual rotation time of the substrate on the plate was more than "x" minutes because the substrate was not under the plasma jet at all times. It was essential to establish a relationship between the rotation time of substrates and the actual CAPP treatment time before start of bacterial inactivation experiments. It was also essential to establish the average time spent by the substrate

under the plasma jet in one rotation as different points on the substrate would be exposed to different times under the plasma jet due to varying angular displacement covered by each point. Figure 18 a) represents a schematic of substrate on a rotating plate under the plasma jet, Figure 18 b) is a focused illustration depicting CAPP jet circle of influence estimation, and Figure 18 c) is a focused illustration of the substrate in a petri dish passing inside the CAPP jet – circle of influence.

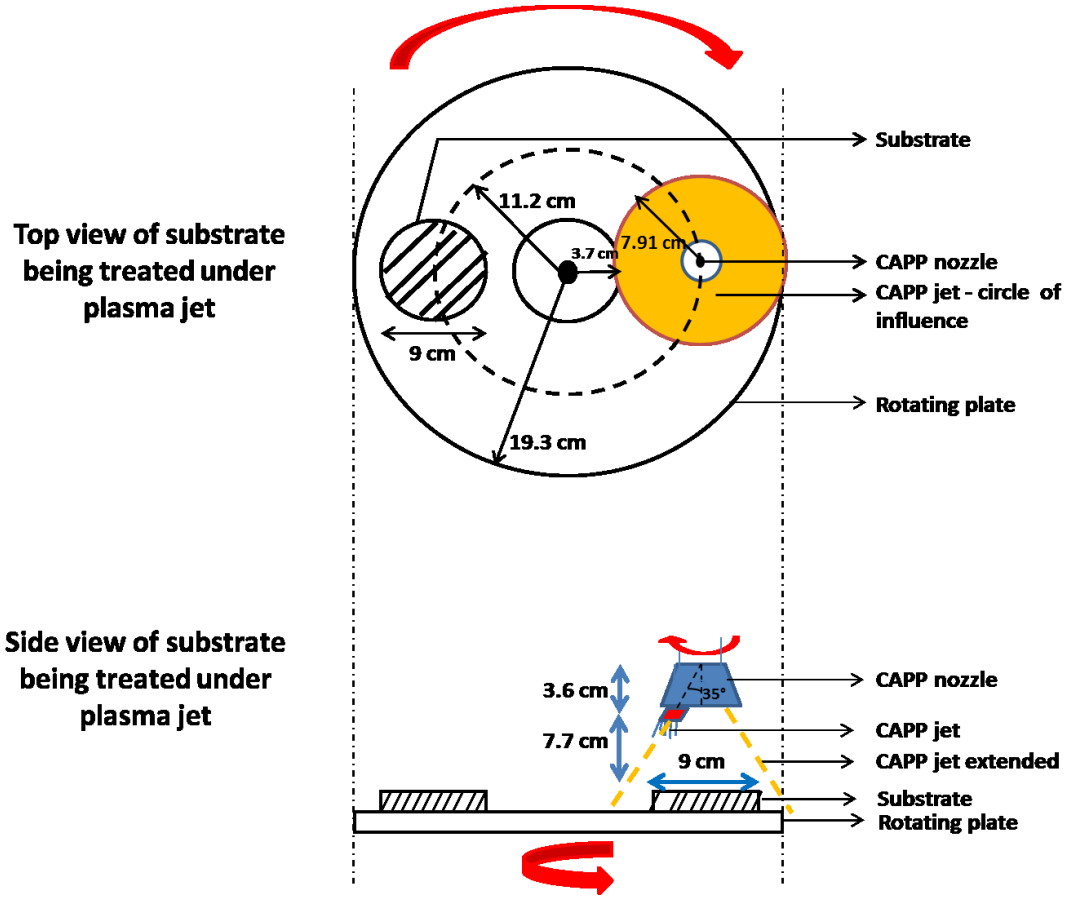

Figure 18 a: Schematic of substrate in a petri dish on a rotating plate under the plasma jet (not drawn to scale)

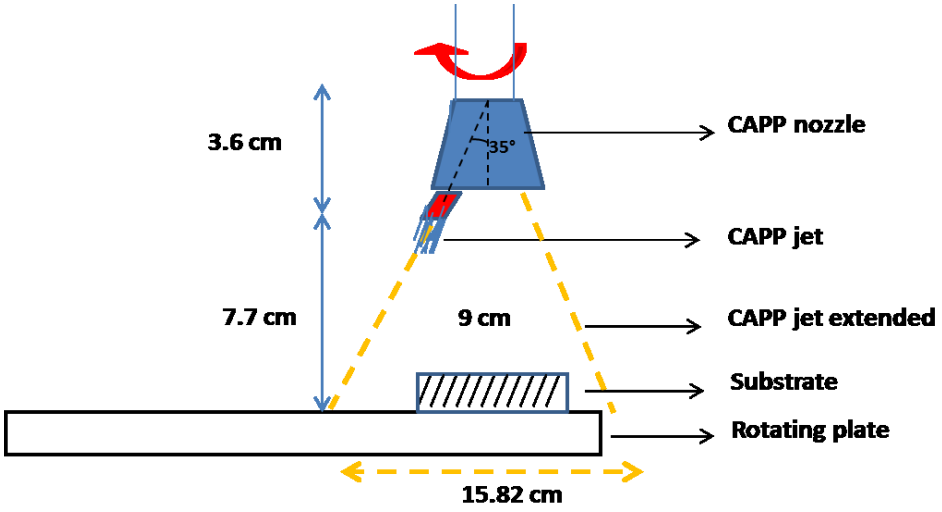

Figure 18 b: Illustration depicting CAPP jet circle of influence estimation (not drawn to scale)

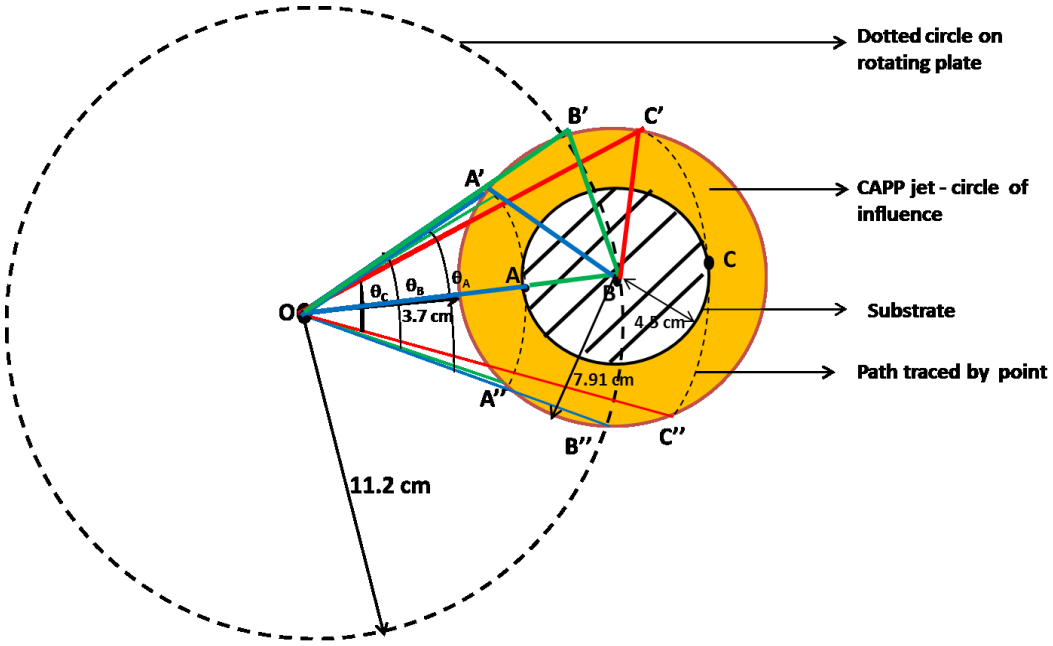

Figure 18 c: Illustration of substrate in a petri dish passing inside the CAPP jet – circle of influence (not drawn to scale)

As seen in Figure 18 a, substrate i.e. a petri dish of 9 cm diameter was placed on a rotating plate under the CAPP jet. The rotating plate was positioned under the CAPP jet in such a way that the center of the plasma nozzle traced the dotted circle on the rotating plate. Petri dish was oriented such that its center coincided with dotted circle on the rotating plate.

It was ensured that each point on the substrate in the petri dish was exposed to plasma because the CAPP jet circle of influence was larger than the petri dish (Figure 18 b and 18 c). As seen in Figure 18 b, the line passing through the center of the plasma jet was aligned at an angle of 35° to the plasma nozzle. The length of plasma nozzle was 3.6 cm and the substrate was kept at a distance of 7.7 cm from the tip of the plasma nozzle. Thus, the radius of CAPP jet circle of influence = (7.7 cm + 3.6 cm) * tan 35° = 7.91 cm and diameter = 15.82 cm while the radius of the substrate i.e. petri dish was just 4.5 cm.

Figure 18 c explains calculation of average CAPP exposure time of substrate and its relation to the actual rotation time of the rotating plate. Three points on the substrate were considered with A being the point which would spend the maximum time under the CAPP jet circle of influence, B is the center point of the substrate, and C being the point that would spend the least time under the CAPP jet circle of influence. The paths covered by these points under the CAPP jet circle of influence are marked as A'-A -A'' , B'-B-B'', and C'-C-C'' for A, B, and C, respectively. The angular velocity (ω) of all the

three points with respect to center 'O' would be constant. The speed of the rotating plate was set to 30 rpm. Thus, the angular velocity was π rad/s.

Time spent by point A under the plasma jet circle of influence = Angular displacement of point A in 1 rotation (θ_A) / Angular velocity (ω). Angular displacement of A was determined to be 88° = 0.49 π rad using the cosine rule in triangle OA'B (Figure 18 c). Thus the time spent by point A in 1 rotation (θ_A) of substrate under the CAPP jet circle of influence = 0.49 π rad / π rad/s = 0.49 s. Similarly, time spent by point B under the CAPP jet circle of influence in 1 rotation = 0.46 s (triangle OB'B), and time spent by point C under the CAPP jet circle of influence in 1 rotation = 0.32 s (OC'B).

For the sake of simplicity, we have assumed that the time spent by the substrate in the petri dish in 1 rotation is the average of the times spent by these three points. Thus time spent by the substrate under CAPP jet circle of influence in 1 rotation = (0.49 + 0.46 + 0.32)/ 3 s = 0.42 s.

In order to determine CAPP treatment time, preliminary experiments were performed where *E. aerogenes* was subjected to CAPP treatment for varying times from 30 s to 10 min and the microbial inactivation for each time was observed. Overnight *E. aerogenes* culture was grown following protocol explained in section 2.2.5. Once the overnight

culture was ready, it was serially diluted and plated onto MacConkey agar. The MacConkey agar plates were immediately exposed to CAPP for different treatment times, incubated at 37 °C for 18 h, counted and compared against inoculated untreated controls. It was observed that the microbial inactivation increased as the treatment time increased. A treatment time of 8 minutes 12 seconds was selected to make CAPP treatment industrially feasible and to also ensure high level of inactivation.

Thus, in 1 rotation of the rotating plate which takes 2 s, the plate gets exposed for 0.42 s. In order to get an exposure time of 492 s, we need to rotate the plate for 2342.85 s = 39 min, 4 s.

2.2.3. Preparation of overnight bacterial culture for inoculation

Bacteria were scooped out from the glycerol stock using a sterile loop and quadrant streaked onto a Difco Tryptic Soy Agar plate enriched with nalidixic acid at 50 µg/ml concentration. The plate was then incubated at 37 °C for 18 h. A single colony was picked from TSA plate and grown in 10 ml of Bacto Tryptose Phosphate Broth containing nalidixic acid (50 µg/ml) at 37 °C for 18 h. The broth was then split into 1 ml micro centrifuge tubes, bacteria were sedimented by centrifugation (Fisher Scientific accuSpin Micro 17, 5000 rpm, 5 min), washed three times in Difco Peptone Water and resuspended into 1 ml of peptone water. This suspension was used for all the bacterial

inoculation procedures. Cell count of the bacterium was determined via serial dilutions of the cell suspension and subsequent enumeration on nalidixic acid (50 µg /ml) enriched BBL MacConkey Agar and was approximately 10^9 CFU/ml.

2.2.4. Preliminary experiments on sandpapers and fruit surfaces

Preliminary experiments on sandpapers included confirming absence of nalidixic acid resistant *E. aerogenes*, and confirming non-toxicity of sandpapers to *E. aerogenes*. To confirm absence of nalidixic acid resistant *E. aerogenes* on the sandpapers, a sandpaper disc of diameter 9 cm from each of the grit was taken, placed in a stomacher bag containing 49 ml of peptone water, agitated for 3 minutes, performed serial dilutions using peptone water and appropriate dilutions were plated onto nalidixic acid enriched MacConkey Agar (50 µg /ml) . Each experiment was repeated twice to ensure repeatability of results. It was found that presence of any inherent nalidixic acid resistant *E. aerogenes* on sandpapers was below detectable limit. Non toxicity of sandpapers to *E. aerogenes* was ensured when acceptable microbial recoveries of approximately 7 log CFU/sandpaper were attained from sandpaper surfaces from initial microbial inoculation of approximately 9 log CFU/sandpaper (see section 2.2.5. Experimental design and microbiological analysis - inoculated untreated control samples).

Preliminary experiments on fruit surfaces included confirming the absence of nalidixic acid resistant *E. aerogenes* on the fruit peels. A fruit from each variety was taken, peeled using a standard peeler, peels were put in a stomacher bag containing 49 ml of Peptone water, agitated for 3 minutes, serial dilutions were performed using peptone water and appropriate dilutions were plated onto nalidixic acid enriched MacConkey Agar (50 µg /ml). Each experiment was repeated twice to ensure repeatability of results. It was found that presence of any inherent nalidixic acid resistant *E. aerogenes* on fruit surfaces was below detectable limit.

2.2.5. Experimental design and microbiological analysis

Sandpapers were cut in 9 cm diameter circles and taped (from below) inside 9 cm diameter petri dishes (Figure 19). One ml of the bacterial culture was spot inoculated at several different locations on the sandpapers ensuring that the inoculum did not flow to the sides of the sandpapers. Inoculated samples were left to dry for two hours in a biosafety cabinet at room temperature. The dried samples were then treated with CAPP for exposure time of eight minutes twelve seconds at a distance of 7.7 cm from the nozzle, followed by a microbiological analysis of the samples. Temperature was continuously monitored during CAPP treatment using alcohol based thermometer and a thermocouple and the temperature never exceeded 50 °C.

The inoculated untreated control samples (to estimate initial attached bacterial population) and inoculated CAPP treated samples were subjected to microbiological analysis. The samples were transferred to separate sterile stomacher bags with 49 ml of peptone water and homogenized for 3 minutes. One ml of the resulting suspension was serial diluted in 9 ml sterile peptone water tubes. The surviving *E. aerogenes* population was determined by plating appropriate dilutions on nalidixic acid enriched MacConkey Agar (50 µg /ml), incubating at 37 °C for 18 h and enumerated.

Similar procedures for microbial inoculation, plasma treatment and microbial analysis were followed using *E. aerogenes* for fruits surfaces, the only difference being that the fruits were peeled and superglued (Loctite Adhesives, Westlake OH) onto petri dishes with peel surface facing up and peel covering the entire petri dish (Figure 19).

Experiments were repeated three times for sandpapers and seven times for fruit surfaces to ensure repeatability of experimental data. Also, the cell count in the original bacterial suspension used for inoculation was enumerated as a control for each experiment.

Figure 19 illustrates inoculated sandpapers (Grit 600, Grit 400, Grit 280) and fruit peels (golden delicious apple, sunkist valencia orange, cantaloupe) in petri dishes.

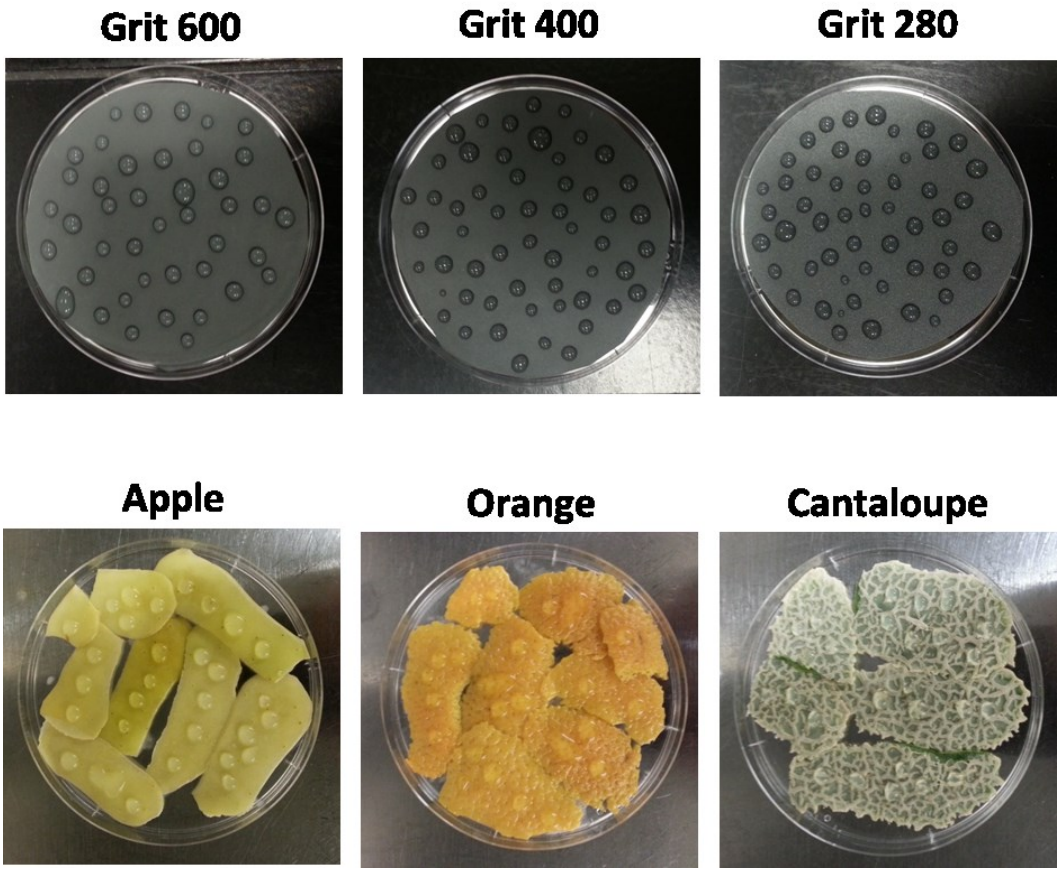

Figure 19: Inoculated sandpapers (Grit 600, Grit 400, and Grit 280) and fruit peels (golden delicious apple, sunkist valencia orange, and cantaloupe) in petri dishes

2.2.6. Instrumental Analysis

Scanning electron microscopy (SEM):

Sandpapers were analyzed for the uniformity of grain stacking using a Scanning Electron Microscope (Zeiss Sigma Field Emission SEM with Oxford EDS, Jena, Germany). Each

sandpaper was cut into a 1 cm x 1 cm piece, sputter coated with gold and analyzed at an accelerating voltage of 10 kV and magnification of 500 X.

Sandpapers inoculated with *E. aerogenes* were also analyzed using Scanning Electron Microscope to confirm the presence of bacteria in between the grains. 1 cm x 1 cm piece of each sandpaper was taken, spot inoculated with a drop of *E. aerogenes* culture, dried in a biosafety cabinet for two hours, and fixed with 4% paraformaldehyde solution made in Phosphate Buffered Saline (PBS) for 30 minutes. The sample was then washed two times with PBS, dehydrated in a freeze dryer (Labconco 1 Liter Benchtop Freeze Dry System, Kansas City, MO) for 8 h, and imaged using the SEM at an accelerating voltage of 10 kV and magnification of 1000 X and 2000 X.

Confocal laser scanning microscopy

Surface roughness of the sandpapers and the fruits was measured using Leica TCS SPII Confocal Microscope (Buffalo Grove, IL) adapting the protocol established by (Sheen et al., 2008). Samples were mounted on the universal stage on slides and then illuminated using 488 nm Argon-Krypton Laser. Reflection from sample surfaces was collected with a long working distance (2.2 mm) 10X lens (numerical aperture = 0.40) in a single, 8 bit channel and 1.00 P AU pinhole; begin and end limits of the vertical series were set visually in the Z-wide scan control. Four pixel lines were averaged in each optical

section. Each frame was 1024 * 1024 pixels. Image stacks with the optimal number of sections for maximal z-resolution (for the lens) were transformed into topographical images for measurements in the Leica LCS Materials software package.

Roughness was quantified using the roughness parameter of Pq (Equation 2) which is the root mean square deviation of the assessed primary profile (ISO 4287-1997, (Mattsson et al., 2008; Standardization, 1997)). Primary profile as explained earlier (section 1.2.) is the actual measured surface profile along the line segment.

$$Pq = \sqrt{\left(\frac{1}{l}\right) * \int_0^l z^2(x)dx} \qquad \text{(Equation 2)}$$

Where l is the evaluation length, z is peak or valley height at every point (x) along the length. Pq has a unit of µm.

For each sandpaper grit, Pq value was an average of assessment of a total of 30 profiles, with fifteen profiles each on two different sandpapers. For each fruit type, Pq value was an average of assessment of a total of 36 profiles, with 12 profiles each on three fruits.

Optical emission spectroscopy

A Black-Comet UV-VIS Spectrometer (StellarNet Inc., Tampa, USA) was used in conjunction with Atomic Spectra Database from the National Institute of Standards and

Technology to identify and relatively quantify the reactive species in the air-plasma jet system (Surowsky et al., 2014b). The UV-VIS Spectrometer was equipped with a F400-UV–vis-SR fiber optic in the range from 190 nm to 850 nm and a collimating lens QCol to monitor UV-A (320 nm – 400 nm), UV-B (280 nm – 320 nm) and UV–C radiation (200 nm – 280 nm), as well as the presence of atomic oxygen (777.5 nm) and OH radicals (309 nm). The distance between the detector and plasma was 7.7 cm in the axial direction. Keeping the axial distance at 7.7 cm, measurements were made radially in a plane, starting from the center of the plasma nozzle/substrate and taking measurements at each centimeter up to 5 cm from the center (Figure 17). Each measurement was performed three times with an integration time of 10000 ms and was recorded as emission spectra. The spectral peaks were then identified and processed by using the SpectrWiz software and National Institute of Standards and Technology for Atomic Spectra Database (Kramida, 2014).

2.2.7. Statistical analysis

The surface roughness (Pq) values of sandpapers and fruit surfaces, and log reductions in *E. aerogenes* following CAPP treatment were subjected to one way analysis of variance (ANOVA) and means were compared using Tukey method with a p value of 0.05. Statistical analysis was performed using Minitab 16.2.3 software.

3. RESULTS AND DISCUSSION

3.1. Verification of suitability of model system

To ensure the suitability of the sandpaper model system being used in this research study, two conditions had to be met – i) The model system had to possess a uniform and quantifiable topography. One of the research objectives was to isolate and investigate the effect of surface roughness on microbial inactivation efficacy of CAPP, and a model system with uniform and quantifiable topography would help the case. ii) The bacteria inoculated on the sandpapers had to be present in between the sandpaper grains and not on top of the grains as only then would the effect of surface roughness on microbial inactivation efficacy of CAPP be seen.

Figure 20 illustrates the uniform grain stacking on sandpapers and differences in the topography between the three sandpapers used which were Grit 600, Grit 400, and Grit 280. Figure 21 illustrates the presence of bacteria in between the groves of Grit 600 and Grit 400 sandpapers.

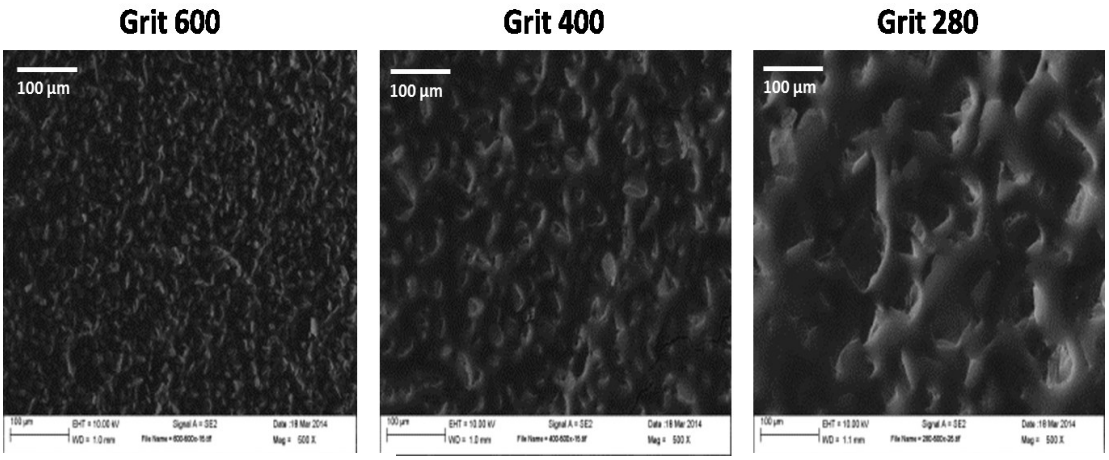

Accelerating Voltage = 10.00 kV; Working Distance = 1.00 mm; Magnification = 500 X

Accelerating Voltage = 10.00 kV; Working Distance = 1.00 mm; Magnification = 500 X

Accelerating Voltage = 10.00 kV; Working Distance = 1.1 mm; Magnification = 500 X

Figure 20: SEM images of grain stacking on three different grits of sandpapers

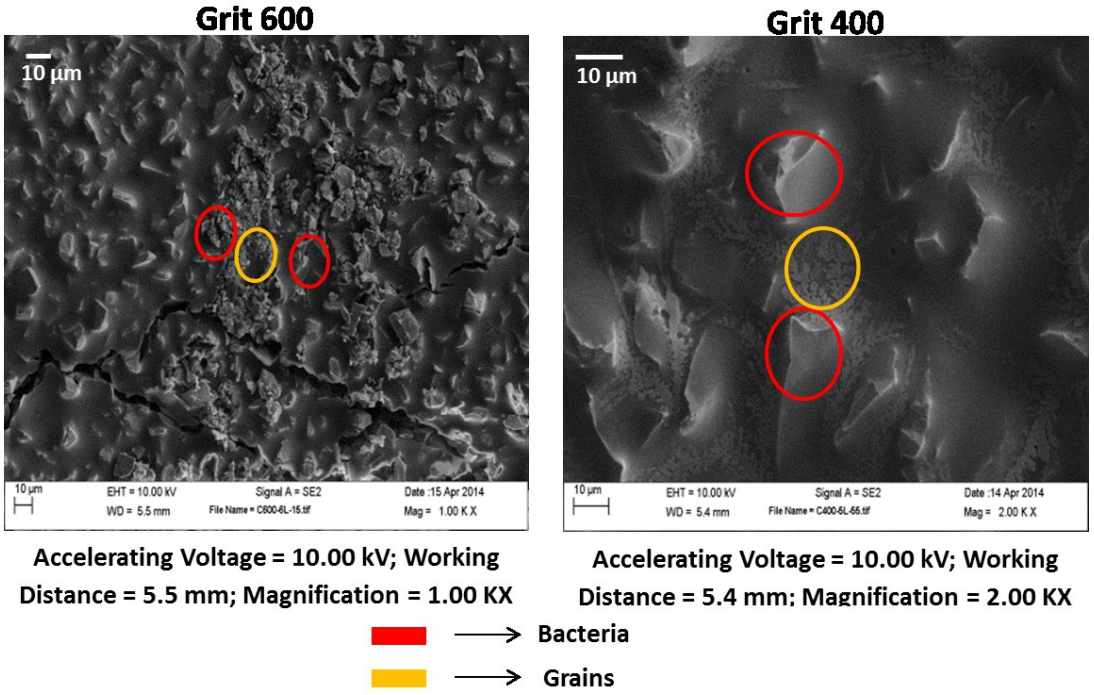

Accelerating Voltage = 10.00 kV; Working Distance = 5.5 mm; Magnification = 1.00 KX

Accelerating Voltage = 10.00 kV; Working Distance = 5.4 mm; Magnification = 2.00 KX

Figure 21: SEM images of Grit 600 and Grit 400 inoculated with *Enterobacter aerogenes*

Thus, the sandpaper model system satisfies both the conditions required to investigate isolated effect of surface roughness on microbial inactivation efficacy of CAPP. Also, by using sandpapers of different grits but made out of the same material as our model system, it was ensured that the variable of different surface energies was eliminated which would have affected the wetting capacity of the bacterial culture, subsequent adhesion of bacteria to the surfaces, and finally the microbial inactivation results (Liu and Zhao, 2005).

3.2. Surface roughness determination and roughness comparison between sandpapers and fruit surfaces

Figure 22 illustrates 750 µm x 750 µm confocal topographical images of Grit 600, Grit 400, and Grit 280 sandpapers along with five of the selected profiles for Pq evaluation. The calculated Pq value using equation 1 along the 5 lines for each sandpaper ranged from 6.71 ± 0.58 µm (for Grit 600) to 16.65 ± 2.53 µm (for Grit 280) with the roughness (Pq) increasing as sandpaper grit size decreased (Table 7). The results were in agreement with the visual observations and the SEM images.

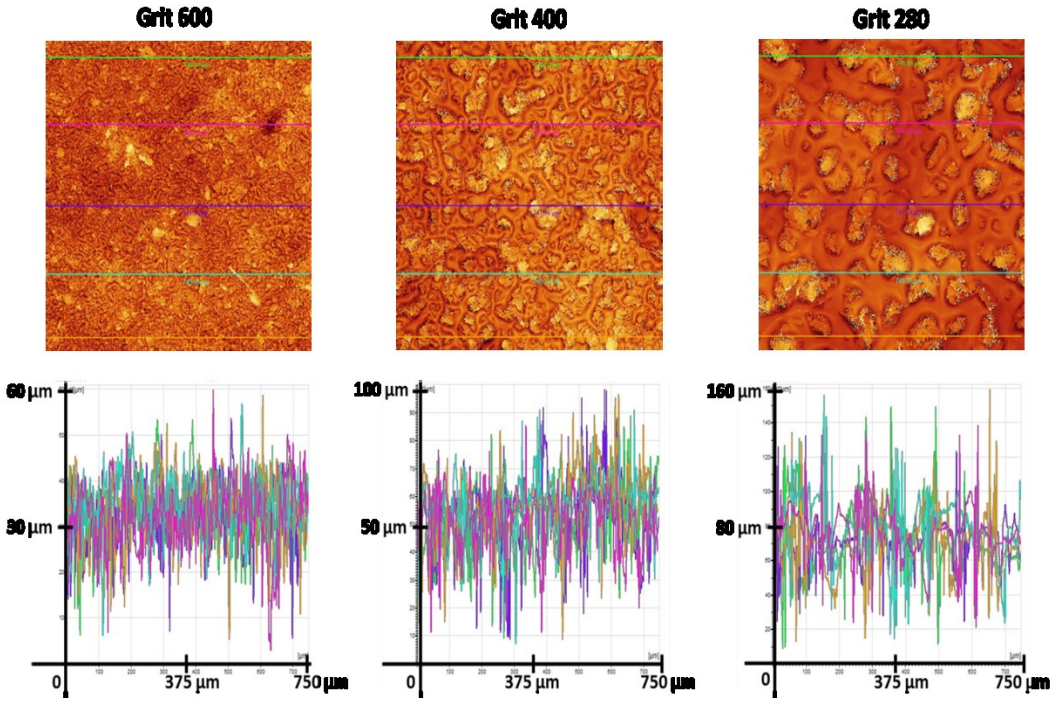

Figure 22: Illustration of 750 µm x 750 µm confocal topographical images of Grit 600, Grit 400, and Grit 280 sandpapers along with five of the selected profiles (lines) for Pq evaluation

Table 7: Sandpaper roughness (Pq) values

Sandpaper Grit Number	**Pq (µm)**
Grit 600	6.71±0.58[a]
Grit 400	11.71±1.18[b]
Grit 280	16.65±2.53[c]

(Data that do not share the same superscript letter are significantly different (Tukey test, $p<0.05$))

Figure 23 illustrates 750 µm x 750 µm confocal topographical images of an apple, an orange, and a cantaloupe surface with three of the selected profiles(lines) for Pq evaluation. The Pq value of fruit surfaces ranged from 6.12 ± 2.88 µm (for apple) to 16.98 ± 6.74 µm (for cantaloupe). Apple surface was the least rough while cantaloupe surface was the roughest (Table 8).

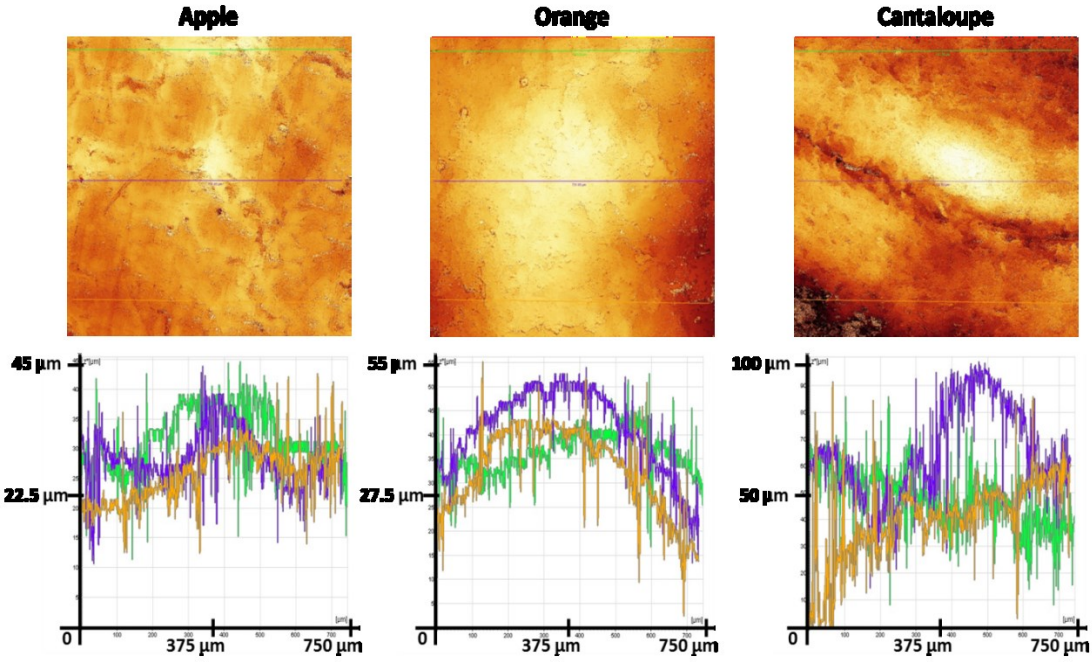

Figure 23: Illustration of 750 µm x 750 µm confocal topographical images of an apple, an orange and a cantaloupe surfaces with three of the selected profiles for Pq evaluation.

Table 8: Fruit surfaces roughness (Pq) values

Fruit	**Pq (µm)**
Apple	6.12±2.88[a]
Orange	13.07±5.26[b]
Cantaloupe	16.98±6.74[c]

(Data that do not share the same superscript letter are significantly different (Tukey test, $p<0.05$))

Figure 24 illustrates comparison of roughness values (Pq) between the sandpapers and fruits used. CLSM results indicated similar roughness (Pq) values for an apple (Golden delicious, variety 4020) and Grit 600, for an orange (Sunkist Valencia, variety 4020) and Grit 400, and for a cantaloupe (variety 4050) and Grit 280. An important thing to note would be the high variability in the roughness values of fruit surfaces indicating the complexity of a real world system.

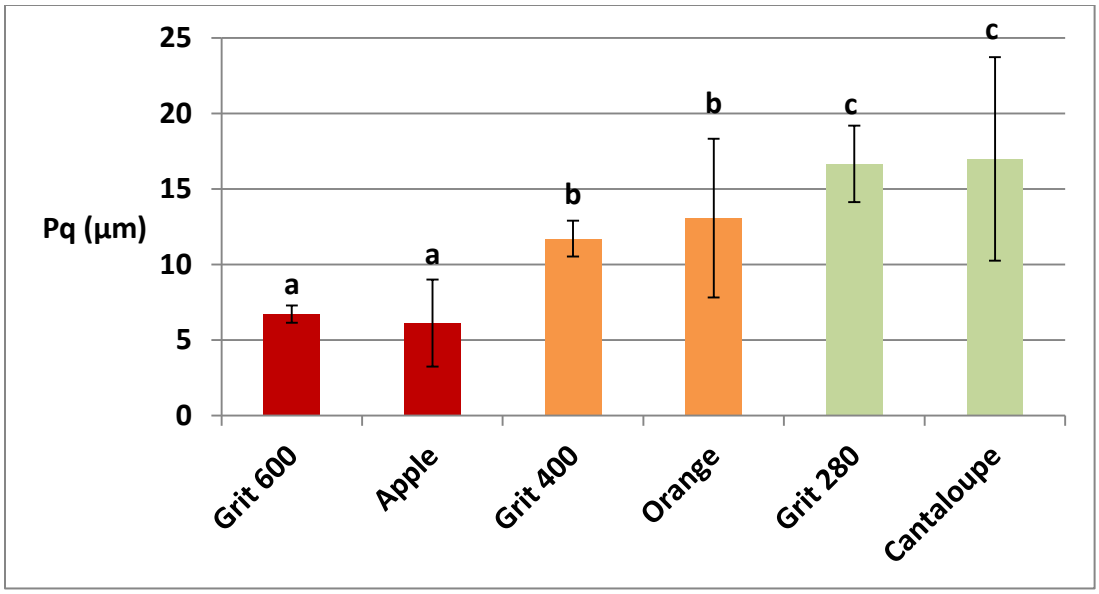

(Vertical bars indicate standard deviation; Data that do not share the same letter are significantly different from each other (Tukey test, $p<0.05$))

Figure 24: Comparison of roughness (Pq) values between the sandpapers and fruits used.

3.3. Effect of CAPP on *E. aerogenes* inoculated on sandpapers

Reduction in *E. aerogenes* on sandpapers post CAPP treatment is represented in Figure 25. The average initial attached populations of *E. aerogenes* on Grit 600, Grit 400, and Grit 280 sandpapers were 6.86 ± 0.09, 6.94 ± 0.26, and 6.79 ± 0.26 log CFU/sandpaper (circular disc of 9 cm diameter), respectively. After treatment with CAPP for 8 minutes 12 seconds, the microbial population reduced by 2.08 ± 0.2, 1.86 ± 0.12, and 1.56 ± 0.18 log CFU for Grit 600, Grit 400 and Grit 280, respectively, with a significant difference in

log reduction between Grit 600 and Grit 280 ($p<0.05$). Thus, it can be concluded that the microbial inactivation decreased as the roughness of sandpapers increased.

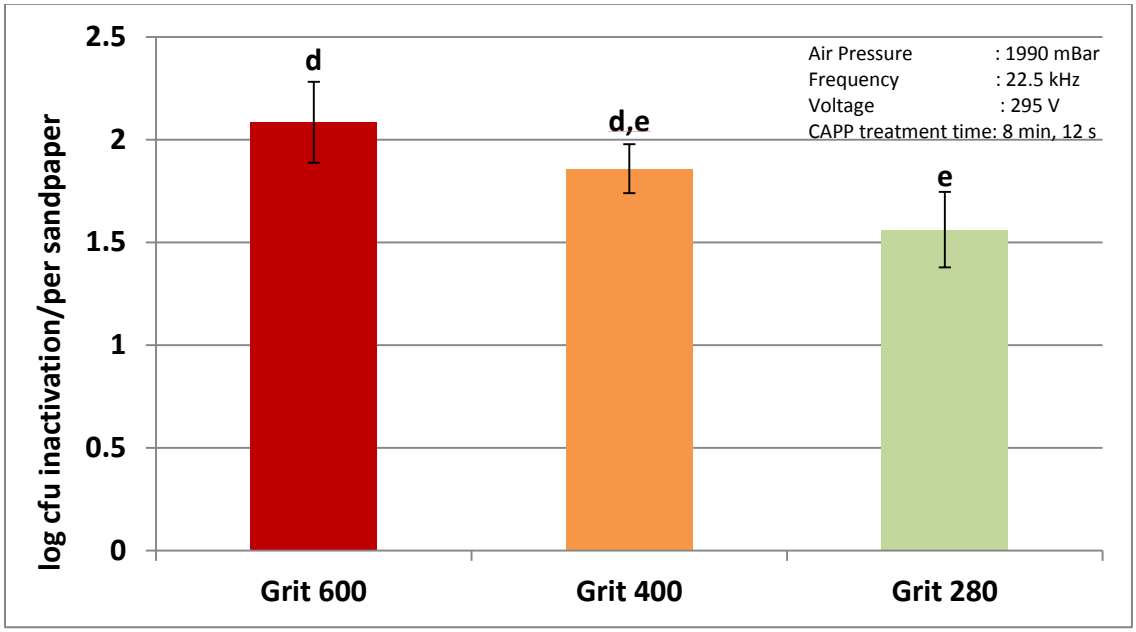

(Vertical bars indicate standard deviation; Data that do not share the same letter are significantly different from each other (Tukey test, $p<0.05$), n=4)

Figure 25: Inactivation of *Enterobacter aerogenes* on sandpapers

The microbial inactivation results from sandpaper experiments showed that in a scenario where surface roughness is the only parameter of difference, the microbial inactivation efficacy of CAPP would be affected by the surface roughness and the inactivation would decrease with increasing surface roughness. These results fulfill the first objective of this research study which was to isolate and investigate the effect of surface roughness on microbial inactivation efficacy of CAPP.

3.4. Effect of CAPP on *E. aerogenes* inoculated on fruit surfaces

Reduction in *E. aerogenes* on fruit surfaces post CAPP treatment is represented in Figure 26. The average initial attached population of *E. aerogenes* on apple, orange and cantaloupe peels were 6.81 ± 0.36, 6.18 ± 0.86, 7.29 ± 0.46 log CFU/fruit, respectively. After treatment with CAPP for 8 minutes 12 seconds the microbial populations reduced by 1.86 ± 1.27, 0.77 ± 0.86, 0.61 ± 0.78 log CFU for the apple, the orange, and the cantaloupe, respectively, with a significant difference in log reduction between apple and cantaloupe ($p<0.05$). The microbial inactivation decreased as the fruit surface roughness increased similar to the results of sandpapers. An important point to note here is the high variability in microbial inactivation on fruit surfaces, as compared to the inactivation on sandpapers. This can be attributed to high variability in their roughness (Pq) values as mentioned earlier and it gives a first insight into the complexity involved in the real world and suitability of CAPP for fresh produce decontamination.

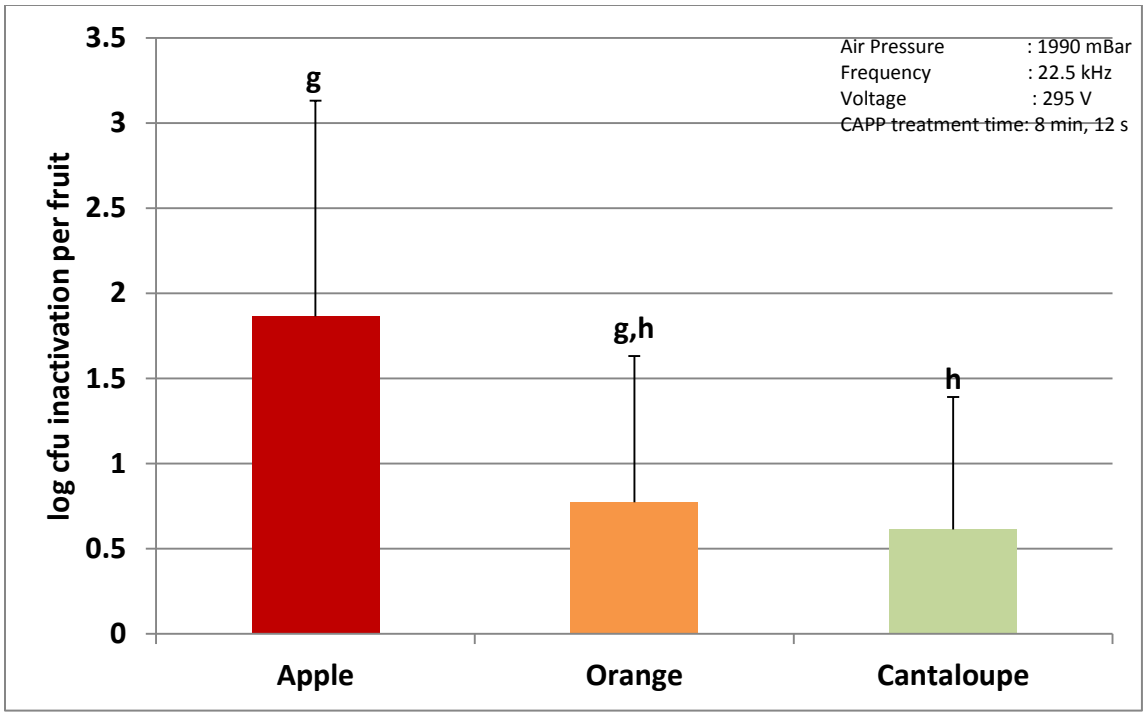

(Vertical bars indicate standard deviation; Data that do not share the same letter are significantly different from each other (Tukey test, $p<0.05$), n=8)

Figure 26: Inactivation of *Enterobacter aerogenes* on fruit surfaces

3.5. Microbial inactivation comparisons between sandpapers and fruit surfaces

The reason for selecting fruits and sandpapers with similar roughness (Pq) values was to be able to show a fair comparison between their microbial inactivation results. Thus, if surface roughness was the governing parameter affecting the microbial inactivation efficacy of CAPP, then the microbial inactivations would be similar between fruits and their corresponding sandpaper grits. On comparison of the microbial inactivations between apple and Grit 600, between orange and Grit 400, and between cantaloupe

and Grit 280, statistically significant differences in microbial inactivations were found between an orange and Grit 400 ($p = 0.034$), and between a cantaloupe and Grit 280 ($p = 0.023$). However, microbial inactivation on an apple and Grit 600 was not statistically significantly different ($p = 0.743$). This shows that surface roughness most likely is not the only governing parameter and there could be other factors which are affecting the microbial inactivation efficacy of CAPP on fresh produce such as those mentioned earlier: moisture content of the surfaces, composition of natural and artificial waxes on the surfaces, migration of microorganisms from the exterior to the interior of the fruits, surface energy of the substrates, etc. The result above fulfilled the second objective of the research study which was to understand the extent to which surface roughness affects the microbial inactivation efficacy of CAPP in fresh produce.

3.6. Identification and relative quantification of reactive species generated in the plasma jet

Figure 27 represents the emission spectrum at different locations (center, 1 cm, 2 cm, 3 cm, 4 cm, 5 cm from center) under the air plasma jet in a plane perpendicular to the jet direction at 7.7 cm from the nozzle. Emission spectrum illustrates the relative concentrations of nitrogen and oxygen ions.

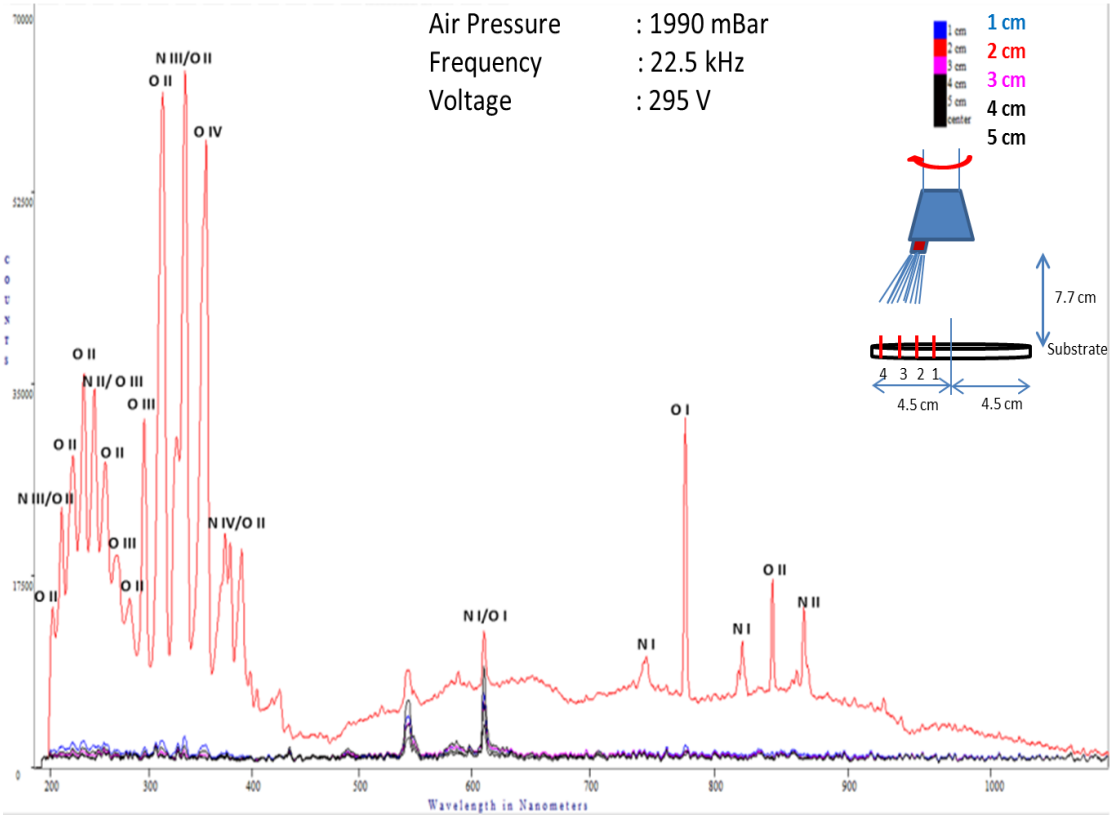

Figure 27: Emission spectra recorded via OES at different locations (center, 1 cm, 2 cm, 3 cm, 4 cm, 5 cm) under the air - plasma jet

Reactive ions were identified based on their observed wavelengths using the Atomic Spectra Database from the National Institute of Standards and Technology (Kramida, 2014). The establishment of a gradient in the concentration of reactive ions can be clearly seen with the ion intensity highest at a distance of 2 cm from the center. This might be due to establishment of air current in the plasma jet and necessitates revolving samples under the plasma jet to ensure uniformity.

Plasma is a high energy and a highly dynamic system. Some of the plasma species generated including superoxide, hydroxyl radical, and peroxynitrite are extremely short lived and have a half-life of less than a second while some like hydrogen peroxide are relatively more stable even up to 24 hours (Devasagayam et al., 2004; HERA, 2005). One research study by Gaens and Bogaerts (2013) reports reaction chemistry set for an argon/humid air mixture, which considers 84 different species and 1880 reactions (Gaens and Bogaerts, 2013). The inactivation achieved by plasma is primarily a result of antimicrobial effects of highly reactive species such as O, OH, NO_2 , $O^{\bullet}$, O_2, O_3, $OH^{\bullet}$, $NO^{\bullet}$, etc. and secondarily due to minimal or indirect effect of UV radiation, via the mechanisms of electrostatic disruption and oxidation of cellular components (Harrison et al., 1997; Kelly-Wintenberg et al., 1999; Laroussi and Leipold, 2004; Misra et al., 2011). In our plasma system, a high intensity of metastable singlet state of oxygen (OI) at around 777.5 nm was recorded, oxygen and nitrogen ions at different energy states were detected which would give way to formation of antimicrobial reactive species via electron impact excitation and dissociation. It was beyond the scope of this research study to elucidate on the reaction chemistry of the charged species and reactive ions being generated which would lead to formation of the antimicrobial species.

4. CONCLUSIONS

Results from sandpaper model system confirmed that surface roughness does play a role in the microbial inactivation efficacy of CAPP and the microbial inactivation decreases as the substrate surface roughness increases. Surface roughness isn't the only governing parameter affecting microbial inactivation efficacy of CAPP on fruit surfaces and this was demonstrated by comparison of model system microbial inactivation results with microbial inactivation results on fruit surfaces having similar roughness values. The results from fruit surfaces showed high variability, and were not predictable from the sandpaper data.

CAPP could be a suitable technique for fresh produce decontamination especially on smoother produce like apples, tomatoes, etc. CAPP achieved inactivation of 1.86 ± 1.27 log CFU of *E. aerogenes* on an apple surface. Further research on CAPP is needed before determining its suitability for fresh produce decontamination. Future research on CAPP needs to be substrate specific, to encompass all factors affecting its microbial inactivation efficacy, and also evaluate its effect on chemical and sensory aspects of the substrate.

5. FUTURE WORK

In order to determine suitability of CAPP for fresh produce decontamination, it is essential to identify, isolate, and quantify the effect of all factors governing its microbial inactivation efficacy, and then develop a predictive microbial inactivation equation encompassing all the factors. It is also important to check the effect of CAPP on the chemical and sensory aspects of fresh produce before designing a decontamination process. It would also be very interesting if a technique of actually quantifying the plasma species is developed. This would lead to a better understanding of the plasma species and their reaction chemistry.

6. REFERENCES

1. Abramzon, N., Joaquin, J.C., Bray, J., Brelles-Marino, G., 2006. Biofilm destruction by RF high-pressure cold plasma jet. Plasma Science, IEEE Transactions on 34, 1304-1309.
2. Australian Microscopy and Microanalysis Research Facility. 2014. MyScope training for advanced research – Scanning Electron Microscopy. Available at http://www.ammrf.org.au/myscope/sem/background/. Accessed on 04/11/2015.
3. Artés, F., Gómez, P., Aguayo, E., Escalona, V., Artés-Hernández, F., 2009. Sustainable sanitation techniques for keeping quality and safety of fresh-cut plant commodities. Postharvest Biology and Technology 51, 287-296.
4. Basaran, P., Basaran-Akgul, N., Oksuz, L., 2008. Elimination of *Aspergillus parasiticus* from nut surface with low pressure cold plasma (LPCP) treatment. Food Microbiology 25, 626-632.
5. B.C. MacDonald & Company, 2010. Basic Components & Elements of Surface Topography. Available at http://www.bcmac.com/pdf_files/surface%20finish%20101.pdf. Accessed on 03/26/2015.
6. Bermúdez-Aguirre, D., Wemlinger, E., Pedrow, P., Barbosa-Cánovas, G., Garcia-Perez, M., 2013. Effect of atmospheric pressure cold plasma (APCP) on the inactivation of *Escherichia coli* in fresh produce. Food Control 34, 149-157.
7. Buajarern, J., Kang, C.-S., Kim, J.W., 2014. Characteristics of laser scanning confocal microscopes for surface texture measurements. Surface Topography: Metrology and Properties 2, 014003.
8. Bussiahn, R., Brandenburg, R., Gerling, T., Kindel, E., Lange, H., Lembke, N., Weltmann, K.-D., von Woedtke, T., Kocher, T., 2010. The hairline plasma: An intermittent negative dc-corona discharge at atmospheric pressure for plasma medical applications. Applied Physics Letters 96, 143701.
9. Cabiscol, E., Tamarit, J., Ros, J., 2000. Oxidative stress in bacteria and protein damage by reactive oxygen species. Int Microbiol 3, 3-8.
10. Carrino, L., Moroni, G., Polini, W., 2002. Cold plasma treatment of polypropylene surface: a study on wettability and adhesion. Journal of Materials Processing Technology 121, 373-382.
11. Center for Disease Control and Prevention, 2015. List of selected multistate fodborne outbreak investigations. Available at http://www.cdc.gov/foodsafety/outbreaks/multistate-outbreaks/outbreaks-list.html. Accessed on 02/23/2015
12. Chemicool, 2014. Definition of Atomic-emission spectroscopy (AES, OES). Available at http://www.chemicool.com/definition/atomic_emission_spectroscopy_aes_oes.html. Accessed on 03/22/2015.

13. d'Agostino, R., Favia, P., Oehr, C., Wertheimer, M.R., 2005. Low-temperature plasma processing of materials: past, present, and future. Plasma Processes and Polymers 2, 7-15.

14. Deng, S., Ruan, R., Mok, C.K., Huang, G., Lin, X., Chen, P., 2007. Inactivation of *Escherichia coli* on almonds using nonthermal plasma. J Food Sci 72, M62-66.

15. Deng, X.T., Shi, J.J., Shama, G., Kong, M.G., 2005. Effects of microbial loading and sporulation temperature on atmospheric plasma inactivation of *Bacillus subtilis* spores. Applied Physics Letters 87, 153901.

16. Denis Semwogerere, E.R.W., 2005. Confocal Microscopy, Encyclopedia of Biomaterials and Biomedical Engineering. Taylor & Francis. Oxon, UK.

17. Devasagayam, T.P., Tilak, J.C., Boloor, K.K., Sane, K.S., Ghaskadbi, S.S., Lele, R.D., 2004. Free radicals and antioxidants in human health: current status and future prospects. J Assoc Physicians India 52, 794-804.

18. Dobrynin, D., Fridman, G., Friedman, G., Fridman, A., 2009. Physical and biological mechanisms of direct plasma interaction with living tissue. New Journal of Physics 11, 115020.

19. Dobrynin, D., Friedman, G., Fridman, A., Starikovskiy, A., 2011. Inactivation of bacteria using dc corona discharge: role of ions and humidity. New Journal of Physics 13, 103033.

20. Dove, J.E., Frost, J.D., Dove, P.M., 1996. Geomembrane microtopography by atomic for microscopy. Geosynthetics International 3, 227-245.

21. Ehlbeck, J., Schnabel, U., Polak, M., Winter, J., von Woedtke, T., Brandenburg, R., von dem Hagen, T., Weltmann, K.D., 2011. Low temperature atmospheric pressure plasma sources for microbial decontamination. Journal of Physics D: Applied Physics 44.

22. Ermolaeva, S.A., Varfolomeev, A.F., Chernukha, M.Y., Yurov, D.S., Vasiliev, M.M., Kaminskaya, A.A., Moisenovich, M.M., Romanova, J.M., Murashev, A.N., Selezneva, II, Shimizu, T., Sysolyatina, E.V., Shaginyan, I.A., Petrov, O.F., Mayevsky, E.I., Fortov, V.E., Morfill, G.E., Naroditsky, B.S., Gintsburg, A.L., 2011. Bactericidal effects of non-thermal argon plasma in vitro, in biofilms and in the animal model of infected wounds. J Med Microbiol 60, 75-83.

23. Engineered Software Incorporation. 2015. Dictionary of terms. Available at http://eng-software.com/products/esi-learning/dictionary-of-terms/. Accessed on 05/11/2015.

24. Fan, X., Sokorai, K.J., Engemann, J., Gurtler, J.B., Liu, Y., 2012. Inactivation of *Listeria innocua, Salmonella* Typhimurium, and *Escherichia coli* O157:H7 on surface and stem scar areas of tomatoes using in-package ozonation. J Food Prot 75, 1611-1618.

25. Food and Agricultural Organization of the United Nations & World Health Organization, 2008. Report on microbiological hazards in fresh fruits and vegetables. Available at http://www.who.int/foodsafety/publications/micro/MRA_FruitVeges.pdf. Accessed on 02/25/2015.

26. U.S. Food and Drug Administration, 2009. Draft Guidance for Industry: Guide to minimize microbial food safety hazards of leafy greens. Available at http://www.fda.gov/Food/GuidanceRegulation/GuidanceDocumentsRegulatoryInformation/ProducePlantProducts/ucm174200.htm. Accessed on 02/25/2015.

27. Fernandez, A., Noriega, E., Thompson, A., 2013. Inactivation of *Salmonella enterica* serovar Typhimurium on fresh produce by cold atmospheric gas plasma technology. Food Microbiology 33, 24-29.

28. Fernández, A., Shearer, N., Wilson, D.R., Thompson, A., 2012. Effect of microbial loading on the efficiency of cold atmospheric gas plasma inactivation of *Salmonella enterica* serovar Typhimurium. International Journal of Food Microbiology 152, 175-180.

29. Fernández, A., Thompson, A., 2012. The inactivation of *Salmonella* by cold atmospheric plasma treatment. Food Research International 45, 678-684.

30. Fridman, G., Brooks, A.D., Balasubramanian, M., Fridman, A., Gutsol, A., Vasilets, V.N., Ayan, H., Friedman, G., 2007. Comparison of direct and indirect effects of non-thermal atmospheric-pressure plasma on bacteria. Plasma Processes and Polymers 4, 370-375.

31. Gaens, W.V., Bogaerts, A., 2013. Kinetic modelling for an atmospheric pressure argon plasma jet in humid air. Journal of Physics D: Applied Physics 46, 275201.

32. Gaunt, L.F., Beggs, C.B., Georghiou, G.E., 2006. Bactericidal action of the reactive species produced by gas-discharge nonthermal plasma at atmospheric pressure: a review. IEEE Transactions on Plasma Science 34, 1257-1269.

33. Carleton College Geochemical Instrumentation and Analysis, 2013. Scanning Electron Microscopy (SEM). Available at http://serc.carleton.edu/research_education/geochemsheets/techniques/SEM.html . Accessed on 02/26/2015.

34. Gil, M.I., Selma, M.V., López-Gálvez, F., Allende, A., 2009. Fresh-cut product sanitation and wash water disinfection: problems and solutions. International Journal of Food Microbiology 134, 37-45.

35. Gil, M.I., Selma, M.V., Suslow, T., Jacxsens, L., Uyttendaele, M., Allende, A., 2015. Pre- and postharvest preventive measures and intervention strategies to control microbial food safety hazards of fresh leafy vegetables. Critical Reviews in Food Science and Nutrition 55, 453-468.

36. Grzegorzewski, F., Rohn, S., Kroh, L.W., Geyer, M., Schlüter, O., 2010. Surface morphology and chemical composition of lamb's lettuce (*Valerianella locusta*) after exposure to a low-pressure oxygen plasma. Food Chemistry 122, 1145-1152.

37. Harrison, S.L., Barbosa-Cánovas, G.V., Swanson, B.G., 1997. *Saccharomyces cerevisiae* structural changes induced by pulsed electric field treatment. LWT - Food Science and Technology 30, 236-240.

38. Human & Environmental Risk Assessment on ingredients of household cleaning products (HERA), 2005. Hydrogen Peroxide Version 1.0. Available at http://www.heraproject.com/files/36-f-05-shor_h2o2_version1.pdf. Accessed on 03/01/2015.

39. Isbary, G., Stolz, W., Shimizu, T., Monetti, R., Bunk, W., Schmidt, H.U., Morfill, G.E., Klämpfl, T.G., Steffes, B., Thomas, H.M., Heinlin, J., Karrer, S., Landthaler, M., Zimmermann, J.L., 2013. Cold atmospheric argon plasma treatment may accelerate wound healing in chronic wounds: Results of an open retrospective randomized controlled study in vivo. Clinical Plasma Medicine 1, 25-30.

40. Jenoptik Inc., 2008. Roughness measuring systems from hommel-etamic –surface texture parameters in practice. Available at http://www.metrology-direct.com/Lib/Docs/Brochures/Surface-Roughness-Parameters.pdf. Accessed on 02/21/2015.

41. Joshi, S.G., Cooper, M., Yost, A., Paff, M., Ercan, U.K., Fridman, G., Friedman, G., Fridman, A., Brooks, A.D., 2011. Nonthermal dielectric-barrier discharge plasma-induced inactivation involves oxidative DNA damage and membrane lipid peroxidation in *Escherichia coli*. Antimicrob Agents Chemother 55, 1053-1062.

42. Keeratipibul, S., Phewpan, A., Lursinsap, C., 2011. Prediction of coliforms and *Escherichia coli* on tomato fruits and lettuce leaves after sanitizing by using artificial neural networks. LWT - Food Science and Technology 44, 130-138.

43. Kelly-Wintenberg, K., Hodge, A., Montie, T.C., Deleanu, L., Sherman, D., Reece Roth, J., Tsai, P., Wadsworth, L., 1999. Use of a one atmosphere uniform glow discharge plasma to kill a broad spectrum of microorganisms. Journal of Vacuum Science & Technology; Technology A 17, 1539-1544.

44. Kim, B., Yun, H., Jung, S., Jung, Y., Jung, H., Choe, W., Jo, C., 2011. Effect of atmospheric pressure plasma on inactivation of pathogens inoculated onto bacon using two different gas compositions. Food Microbiology 28, 9-13.

45. Kim, J.E., Lee, D.-U., Min, S.C., 2014. Microbial decontamination of red pepper powder by cold plasma. Food Microbiology 38, 128-136.

46. Klingspor-Abrasives, 2015. Basics of coated abrasives. Available at http://www.klingspor.com/ref_asktech_coatedabrasivebasics.htm. Accessed on 04/10/2015.

47. Kolattukudy, P.E., 1984. Natural waxes on fruits. Post Harvest Pomology Newsletter 2(2), 3-7.

48. Kramida, A., Ralchenko, Yu., Reader, J., and NIST ASD Team, 2014. NIST atomic spectra database (ver. 5.2), [Online], National Institute of Standards and Technology, Gaithersburg, MD. .

49. Lacombe, A., Niemira, B.A., Gurtler, J.B., Fan, X., Sites, J., Boyd, G., Chen, H., 2015. Atmospheric cold plasma inactivation of aerobic microorganisms on blueberries and effects on quality attributes. Food Microbiology 46, 479-484.

50. Laroussi, M., Leipold, F., 2004. Evaluation of the roles of reactive species, heat, and UV radiation in the inactivation of bacterial cells by air plasmas at atmospheric pressure. International Journal of Mass Spectrometry 233, 81-86.

51. Lee, H.J., Jung, H., Choe, W., Ham, J.S., Lee, J.H., Jo, C., 2011. Inactivation of *Listeria monocytogenes* on agar and processed meat surfaces by atmospheric pressure plasma jets. Food Microbiology 28, 1468-1471.

52. Lee, K., Paek, K.H., Ju, W.T., Lee, Y., 2006. Sterilization of bacteria, yeast, and bacterial endospores by atmospheric-pressure cold plasma using helium and oxygen. J Microbiol 44, 269-275.

53. Liu, Y., Zhao, Q., 2005. Influence of surface energy of modified surfaces on bacterial adhesion. Biophysical Chemistry 117, 39-45.

54. Loeb, L.B., 1960. Basic processes of gaseous electronics. University of California Press, Berkeley, USA.

55. Loeb, L.B., Meek, J.M., 1940. The mechanism of spark discharge in air at atmospheric pressure. Journal of Applied Physics 11, 438-447.

56. Machala, Z., Janda, M., Hensel, K., Jedlovský, I., Leštinská, L., Foltin, V., Martišovitš, V., Morvová, M., 2007. Emission spectroscopy of atmospheric pressure plasmas for bio-medical and environmental applications. Journal of Molecular Spectroscopy 243, 194-201.

57. Mary S. Palumbo, J.R.G., David E. Gombas, Larry R. Beuchat, Christine M. Bruhn, Barbara Cassens, Pascal Delaquis, Jeffrey M. Farber,Linda J. Harris, Keith Ito, Michael T. Osterholm, Michelle Smith,and Katherine M.J. Swanson, 2007. Recommendations for handling fresh-cut leafy green salads by consumers and retail foodservice operators. Food Protection Trends 27, 892-898.

58. Mattsson, L., Bolt, P., Azcarate, S., Brousseaud, E., Fillon, B., Fowler, R., Gelink, E., Griffiths, C., Khan Malek, C., Marson, S., Retolaza, A., Schneider, A., Schoth, A., Temun, A., Tosello, G., Mattsson, L., Bolt, P., Azcarate, S., Brousseaud, E., Fillon, B., Fowler, R., Gelink, E., Griffiths, C., Khan Malek, C., Marson, S., Retolaza, A., Schneider, A., Schoth, A., Temun, A., Tosello, G., 2008. How reliable are surface roughness measurements of micro-features?, International Conference on Multi-Material Micro Manufacture. Whittles Publishing, Riga (Latvia), pp. 139-142.

59. Meichsner, J., 2005. Low temperature plasmas, in: Dinklage, A., Klinger, T., Marx, G., Schweikhard, L. (Eds.), Plasma Physics. Springer Berlin Heidelberg, pp. 95-116.

60. Mendis, D.A., Rosenberg, M., Azam, F., 2000. A note on the possible electrostatic disruption of bacteria. Plasma Science, IEEE Transactions on 28, 1304-1306.

61. Merriam-Webster, produce, Merriam-Webster. Available at http://www.merriam-webster.com/dictionary/produce. Accessed on 05/11/2015.

62. Misra, N.N., Moiseev, T., Patil, S., Pankaj, S.K., Bourke, P., Mosnier, J.P., Keener, K.M., Cullen, P.J., 2014. Cold plasma in modified atmospheres for post-harvest treatment of strawberries. Food and Bioprocess Technology, 1-10.

63. Misra, N.N., Patil, S., Moiseev, T., Bourke, P., Mosnier, J.P., Keener, K.M., Cullen, P.J., 2014. In-package atmospheric pressure cold plasma treatment of strawberries. Journal of Food Engineering 125, 131-138.

64. Misra, N.N., Tiwari, B.K., Raghavarao, K.S.M.S., Cullen, P.J., 2011. Nonthermal plasma inactivation of food-borne pathogens. Food Engineering Reviews 3, 159-170.

65. Mitutoyo American Corporation, 2009. Surface roughness measurement. Available at http://www.mitutoyo.com/wp-content/uploads/2012/11/1984_Surf_Roughness_PG.pdf. Accessed on 03/27/2015.

66. Moisan, M., Barbeau, J., Moreau, S., Pelletier, J., Tabrizian, M., Yahia, L.H., 2001. Low-temperature sterilization using gas plasmas: a review of the experiments and an analysis of the inactivation mechanisms. International Journal of Pharmaceutics 226, 1-21.

67. Montenegro, J., Ruan, R., Ma, H., Chen, P., 2002. Inactivation of *E. coli* O157:H7 using a pulsed nonthermal plasma system. Journal of Food Science 67, 646-648.

68. Niemira, B.A., 2012. Cold plasma decontamination of foods. Annu Rev Food Sci Technol 3, 125-142.

69. Niemira, B.A., Sites, J., 2008. Cold Plasma inactivates *Salmonella* Stanley and *Escherichia coli* O157:H7 inoculated on golden delicious apples. Journal of Food Protection 71, 1357-1365.

70. Noriega, E., Shama, G., Laca, A., Díaz, M., Kong, M.G., 2011. Cold atmospheric gas plasma disinfection of chicken meat and chicken skin contaminated with *Listeria innocua*. Food Microbiology 28, 1293-1300.

71. Ölmez, H., Kretzschmar, U., 2009. Potential alternative disinfection methods for organic fresh-cut industry for minimizing water consumption and environmental impact. LWT - Food Science and Technology 42, 686-693.

72. Patil, S., Moiseev, T., Misra, N.N., Cullen, P.J., Mosnier, J.P., Keener, K.M., Bourke, P., 2014. Influence of high voltage atmospheric cold plasma process parameters and role of relative humidity on inactivation of *Bacillus atrophaeus* spores inside a sealed package. Journal of Hospital Infection 88, 162-169.

73. Perni, S., Shama, G., Hobman, J.L., Lund, P.A., Kershaw, C.J., Hidalgo-Arroyo, G.A., Penn, C.W., Deng, X.T., Walsh, J.L., Kong, M.G., 2007. Probing bactericidal mechanisms induced by cold atmospheric plasmas with *Escherichia coli* mutants. Applied Physics Letters 90, 073902.

74. Perni, S., Shama, G., Kong, M.G., 2008a. Cold atmospheric plasma disinfection of cut fruit surfaces contaminated with migrating microorganisms. Journal of Food Protection 71, 1619-1625.

75. Prasad, V., Semwogerere, D., Weeks, E.R., 2007. Confocal microscopy of colloids. Journal of Physics: Condensed Matter 19, 113102.

76. Purdue University, 2014. Scanning electron microscopy. Available at https://www.purdue.edu/ehps/rem/rs/sem.htm/ Accessed on 05/11/2015.

77. Ragni, L., Berardinelli, A., Vannini, L., Montanari, C., Sirri, F., Guerzoni, M.E., Guarnieri, A., 2010. Non-thermal atmospheric gas plasma device for surface decontamination of shell eggs. Journal of Food Engineering 100, 125-132.

78. Reutscher, A., 2001. Characteristics of low temperature plasmas under non-thermal conditions - a short summary, in: Rainer Hippler, H.K., Martin Schmidt, Karl H. Schoenbach (Ed.), Low Temperature Plasma Physics. Wiley-VCH Verlag GmbH, Weinheim, pp. 29-54.

79. Richards, G.M., Beuchat, L.R., 2005. Infection of cantaloupe rind with *Cladosporium cladosporioides* and *Penicillium expansum*, and associated migration of *Salmonella poona* into edible tissues. Int J Food Microbiol 103, 1-10.

80. Ringus, D.L., Moraru, C.I., 2013. Pulsed light inactivation of *Listeria innocua* on food packaging materials of different surface roughness and reflectivity. Journal of Food Engineering 114, 331-337.
81. Rød, S.K., Hansen, F., Leipold, F., Knøchel, S., 2012. Cold atmospheric pressure plasma treatment of ready-to-eat meat: Inactivation of *Listeria innocua* and changes in product quality. Food Microbiology 30, 233-238.
82. Schluter, O., Ehlbeck, J., Hertel, C., Habermeyer, M., Roth, A., Engel, K.H., Holzhauser, T., Knorr, D., Eisenbrand, G., 2013. Opinion on the use of plasma processes for treatment of foods. Mol Nutr Food Res 57, 920-927.
83. Scholtz, V., Julák, J., Kříha, V., 2010. The microbicidal effect of low-temperature plasma generated by corona discharge: comparison of various microorganisms on an agar surface or in aqueous suspension. Plasma Processes and Polymers 7, 237-243.
84. Scholtz, V., Pazlarová, J., Soušková, H., Khun, J., Julák, J., 2015. Nonthermal plasma — A tool for decontamination and disinfection. Biotechnology Advances.
85. SeaBeans, Grit Scales. Available at http://www.seabean.com/polish/GritScales.pdf. Accessed on 05/11/2015.
86. Sheen, S., Bao, G., Cooke, P., 2008. Food surface texture measurement using reflective confocal laser scanning microscopy. Journal of Food Science 73, E227-234.
87. International Organization for Standardization, 1997. Softguage basic framework 4287:1997. Available at http://resource.npl.co.uk/softgauges/pdf/Specification.pdf. Accessed on 05/11/2015.
88. Suelí Fischer Beckert, F.J.R., 2012. MSA method application in evaluating of measurement system used to measure the roughness parameter Ra.15th International Conference on Experimental Mechanics, Portugal.
89. Surowsky, B., Fröhling, A., Gottschalk, N., Schlüter, O., Knorr, D., 2014a. Impact of cold plasma on *Citrobacter freundii* in apple juice: inactivation kinetics and mechanisms. International Journal of Food Microbiology 174, 63-71.
90. Tappi, S., Berardinelli, A., Ragni, L., Dalla Rosa, M., Guarnieri, A., Rocculi, P., 2014. Atmospheric gas plasma treatment of fresh-cut apples. Innovative Food Science & Emerging Technologies 21, 114-122.
91. Thirumdas, R., Sarangapani, C., Annapure, U., 2015. Cold Plasma: A novel non-thermal technology for food processing. Food Biophysics 10, 1-11.
92. Tipa, R.S., Middelkoop, B.B., Kroesen, G.M.W., 2012. Cold plasma for bacterial inactivation, International Symposium on Plasma Chemistry.
93. University of Oklahoma - Samuel Roberts Noble Microscopy Laboratory. SEM preparation and equipment. Available at http://www.microscopy.ou.edu/sem-prep.shtml. Accessed on 05/11/2015.
94. van Bokhorst-van de Veen, H., Xie, H., Esveld, E., Abee, T., Mastwijk, H., Nierop Groot, M., 2015. Inactivation of chemical and heat-resistant spores of *Bacillus* and *Geobacillus* by nitrogen cold atmospheric plasma evokes distinct changes in morphology and integrity of spores. Food Microbiology 45, Part A, 26-33.
95. Vesely, P., 2007. Handbook of Biological Confocal Microscopy, 3rd ed. By James B. Pawley, Editor. Springer Science + Business Media, LLC, New York (2006). ISBN 10: 0-

387-25921-X; ISBN 13: 987-0387-25921-5; hardback; 28 + 985 pages. Scanning 29, 91-91.

96. Vleugels, M., Shama, G., Deng, X.T., Greenacre, E., Brocklehurst, T., Kong, M.G., 2005. Atmospheric plasma inactivation of biofilm-forming bacteria for food safety control. Plasma Science, IEEE Transactions on 33, 824-828.

97. Wagner, H.E., Brandenburg, R., Kozlov, K.V., Sonnenfeld, A., Michel, P., Behnke, J.F., 2003. The barrier discharge: basic properties and applications to surface treatment. Vacuum 71, 417-436.

98. Wang, H., Feng, H., Liang, W., Luo, Y., Malyarchuk, V., 2009. Effect of surface roughness on retention and removal of *Escherichia coli* O157:H7 on surfaces of selected fruits. Journal of Food Science 74, E8-E15.

99. Weltmann Klaus, D., Kindel, E., von Woedtke, T., Hähnel, M., Stieber, M., Brandenburg, R., 2010. Atmospheric-pressure plasma sources: prospective tools for plasma medicine, Pure and Applied Chemistry, p. 1223.

100. WorthPoint, 2010. Sandpapers. Available at http://www.worthpoint.com/wp-content/uploads/2010/08/sandpaper.jpg. Accessed on 05/11/2015.

101. Xing-Min, S., Guan-Jun, Z., Xi-Li, W., Ya-Xi, L., Yue, M., Xian-Jun, S., 2011. Effect of low-temperature plasma on microorganism inactivation and quality of freshly squeezed orange juice. Plasma Science, IEEE Transactions on 39, 1591-1597.

102. Zhao, P., Zhao, T., Doyle, M.P., Rubino, J.R., Meng, J., 1998. Development of a model for evaluation of microbial cross-contamination in the kitchen. J Food Prot 61, 960-963.

103. Ziuzina, D., Patil, S., Cullen, P.J., Keener, K.M., Bourke, P., 2014. Atmospheric cold plasma inactivation of *Escherichia coli, Salmonella enterica* serovar Typhimurium and *Listeria monocytogenes* inoculated on fresh produce. Food Microbiology 42, 109-116.

104. Zohm, H., 2005. Physics of “Hot” Plasmas, in: Dinklage, A., Klinger, T., Marx, G., Schweikhard, L. (Eds.), Plasma Physics. Springer Berlin Heidelberg, pp. 75-93.